AN ABSTRACT OF THE THESIS OF

Stephanie J. Harrington for the degree of Master of Science in Civil Engineering presented on September 24, 2004.

Title: U(VI) Transport in Subsurface Materials: Is Two-Site, One-Species Modeling Sufficient?

Abstract approved: Redacted for Privacy

Brian D. Wood

Uranium adsorption to Hanford sediment was studied for various pH, total inorganic carbon concentrations, and total U(VI) concentrations. Both batch and transport studies were done in an attempt to understand the adsorptive trend of U(VI) on Hanford sediment, and the changes in adsorption as both pH and total inorganic carbon concentrations were varied independently. Results from batch experiments were modeled with both linear and nonlinear adsorption isotherms to determine the overall affects of increasing total U to sediment ratios for each set of experimental conditions. For equilibrium conditions, a two-site, two-species surface complexation model described by Waite et al. (1994) was used in FITEQL to fit the adsorption trend seen in results. The model results followed a trend similar to the data, but were not completely accurate. This may be due to inadequate knowledge of the exact number of surface sites available for the adsorption of U as the sediment chemistry is changed during the equilibration process prior to running each experiment. U transport results were fit with the two-site nonequilibrium convection dispersion equation in the code CXTFIT. This model fit only the pH 9, 10mM inorganic carbon data, suggesting that the two site model does not consider all of the relevant processes. With the modeling and experimental results obtained, it is evident that a thorough understanding of not only the aqueous species, but improved understanding of the surface species are needed to create an accurate model for U adsorption.

U(VI) Transport in Subsurface Materials: Is Two-Site, One-Species Modeling Sufficient?

by

Stephanie J. Harrington

A THESIS

submitted to

Oregon State University

in partial fulfillment of
the requirements for the
degree of

Master of Science

Presented September 24, 2004
Commencement June 2005

Master of Science thesis of Stephanie J. Harrington presented on September 24, 2004.

APPROVED:

Redacted for Privacy

Major Professor, representing Civil Engineering

Redacted for Privacy

Head of the Department of Civil, Construction, and Environmental Engineering

Redacted for Privacy

Dean of the Graduate School

I understand that my thesis will become part of the permanent collection of Oregon State University libraries. My signature below authorizes release of my thesis to any reader upon request.

Redacted for Privacy

Stephanie J. Harrington, Author

ACKNOWLEDGEMENTS

The author expresses sincere appreciation to Dr. John Westall and Dr. Scott Brooks for their assistance with FITEQL modeling software and for their professional insight into issues which came about during experimental modeling of data. Thanks to Dr. Jack Istok for his expert opinions and assistance throughout this research. Sincere gratitude goes to Dr. Brian Wood whom provided the author with the opportunity to perform this research, as well as for both his technical and expert advice throughout. The author would also like to acknowledge Mr. Jesse Jones, whom provided both time and assistance with IC data analyses and technical support with issues that came about during KPA analysis, as well as to everyone whom assisted with the running and sampling of batch experiments. Special thanks to my family and friends whom provided an array of support throughout this research.

TABLE OF CONTENTS

TABLE OF CONTENTS (Continued)

Page

TABLE OF CONTENTS (Continued)

LIST OF FIGURES

LIST OF FIGURES (Continued)

LIST OF FIGURES (Continued)

LIST OF TABLES

LIST OF EQUATIONS

ABBREVIATIONS

Br - Bromide
CDE - Convection Dispersion Equation
DI - Deionized water
IC - Ion Chromatograph
ICP - Inductively Coupled Plasma
KHP - Potassium acid phthalate
KPA - Kinetic Phosphorescence Analyzer
TOC - Total Organic Carbon
U - Uranium

SYMBOLS AND TERMINOLOGY

Aq	aqueous phase
C	concentration, usually aqueous phase, (mg/L)
C_o	initial concentration, (mg/L)
c_r	resident aqueous phase concentration, (mg/cm^3)
D	dispersion coefficient, (cm^2/min)
f	fraction of exchange sites that are always at equilibrium, dimensionless
I	ionic strength, molar
k_1	first order adsorption rate constant, ($cm^3/mg\ min$)
k_{-1}	first order desorption rate constant, (1/min)
K_d	empirical distribution constant, (cm^3/mg)
K_{eq}	aqueous and solid phase equilibrium constant, (L/g)
K_f	Freundlich adsorption coefficient, (L/g)
M	molar concentration
n	empirical Freundlich coefficient, dimensionless
ppm	parts per million (mg/L)
Q	flow rate, (ml/min)
R	retardation factor, dimensionless
S	adsorbed concentration, (mg/g)
s_k	kinetically controlled surface concentration, (mg/mg)
t	time, (min)
v	pore-water velocity, (cm/min)
x	position, (cm)

Greek

α	first-order kinetic rate coefficient, (1/min)
β	partitioning coefficient, dimensionless
ω	mass transfer coefficient, dimensionless
θ	porosity, dimensionless
ρ_b	bulk density, (mg/cm^3)

U(VI) Transport in Subsurface Materials: Is Two-Site, One-Species Modeling Sufficient?

1. INTRODUCTION

Uranium mobility in subsurface environments is of great interest due to high levels of contamination from processing, use, and poor disposal practices, as well as its hazardous decay products. Of particular concern is U(VI) (the mobile valence state of U under oxic conditions) which poses a threat to drinking water and the environment. Studies of the transport mechanisms, surface interactions, and environmental conditions, such as pH, subsurface mineral content, and available anions and cations in the groundwater, have been done to gather a more detailed understanding of how U(VI) interacts in subsurface environments. Various models have been proposed to describe which species are responsible for U surface complexation, particularly with iron minerals. Differences among the models include the major types of uranyl-carbonate surface complexes that adsorb, and the number of sites reacting to form each surface complex.

In this thesis, the results of varying pH and inorganic carbon concentration on U(VI) adsorption to Hanford sediment have been explored. Both batch and column studies were performed under similar conditions, with models being used to fit the resulting data and to predict the aqueous and surface species formed. The two main goals of this work were (1) understanding whether or not conventional "one-species, two-site" models are accurate for this research and (2) to independently examine effects of pH and inorganic carbon concentration on adsorption of U in Hanford sediments.

There were three main hypotheses when beginning this research. The first hypothesis was that changes in pH from alkaline to the acidic range would affect the adsorption of U. It was assumed that in the alkaline pH range U-carbonate species would be dominant, leading to potentially less adsorption; in the acidic pH range U would predominantly be UO_2^{2+}, which would potentially increase adsorption; and finally, with the reduction of pH, mineral phases may be removed from the surface of the sediment leading to a potential increase in available adsorption sites for U. The second hypothesis was that changes in inorganic carbon from high concentration (10mM) to low

concentration (1mM) would affect the adsorption of U. The theory behind this hypothesis included the assumptions that, with the reduction in inorganic carbon concentration, there may be an increase in adsorption due to (a) competition between surface sites and inorganic carbon for the complexation of U; (b) removal of solid mineral carbon phases during sediment equilibration leading to an increase in potential U adsorption sites; and (c) lower ionic strength with the decrease in inorganic carbon concentration, leading to potentially more adsorption. The third and final hypothesis was that the presence of multiple mineral phases may affect the adsorption of U. Research has shown that iron oxy-hydroxides and silica oxides will adsorb U, as well as potentially other mineral phases present in Hanford sediment (Barnett et al. 2002; Bostick et al. 2002; Barnett et al. 2000; Waite et al. 1994; Hsi and Langmuir 1985).

In this study, batch and transport experiments were conducted using Hanford sediment obtained from a site in Richland, WA. Each experiment was conducted at set pH and inorganic carbon concentrations in a closed oxic environment to determine the effects each of these parameters had on the adsorption of U. The resulting U data was analyzed, and then fit using both aqueous and surface speciation diagrams. Batch studies were analyzed with both linear and Freundlich adsorption isotherms to determine the effects of increasing U concentrations on the adsorptive properties of the sediment. Both isotherms fit the data well, with the Freundlich isotherm being slightly better fit. This reinforced the third hypothesis, stated in the above paragraph, that multiple sites and species may be responsible for the adsorption process with this sediment. U breakthrough curves were fit using the two-site nonequilibrium model in CXTFIT. The model fit the pH 9, 10 mM inorganic carbon data very well, but a single chemical species model was not able to accurately fit breakthrough curves from the other three transport experiments.

Aqueous and surface speciation diagrams were created for all experiments. Aqueous speciation diagrams, created with MINEQL+ and using thermodynamic data from Grenthe et al. (1992), were used to provide an idea of which species were being formed in the aqueous phase of each experiment. These simulations showed the accumulation of calcium and silica species in the batch experiments, which form aqueous

and potentially adsorbed calcium-U complexes. In the transport experiments, calcium and silica were present in much lower concentrations, leading to negligible concentrations of the associated complexed species. FITEQL was used to model the combined aqueous and surface speciation for each transport and batch experiment. This model showed a different trend in U adsorption from the experimental results, with the major difference being the pH 4 experiments. The model could potentially be improved by additional information, particularly (1) improved knowledge of the exact number of strong and weak surface sites on the sediment after the sediment equilibration process to the experimental conditions being studied, and (2) improved knowledge about the influence of calcium-U and silica-U surface and aqueous reactions that were not included in the model. For the column experiments, it is hypothesized that as the pH and inorganic carbon were adjusted, solid carbonate and silicate minerals were dissolved from the sediment surface, potentially leaving more reactive sites available for U complexation.

A more detailed discussion of how batch and transport experiments were run, the types of analyses performed, and the results from experiments and modeling are discussed in detail in the following report. Included is an overview of prior research that has been conducted in this area, predictions of which species are responsible for U adsorption, and how well this information fit the results from this study. Hypotheses and conclusions have been made, as well as descriptions of areas where further information is needed for a better understanding of the experimental systems analyzed in this study. This research has shown that U(VI) adsorption increases with the reduction in either equilibrium pH or inorganic carbon concentrations (in alkaline solutions), and that for some geochemical conditions, multi-species geochemical models may be needed to more accurately represent the transport of U in porous media.

2. LITERATURE REVIEW

2.1. Uranium Complexation

Due to the vast number of species that U forms with numerous elements, and associated changes in reactivity depending upon this distribution, determination of particular chemical species formed in the subsurface environments is of great importance. With the use of chemical equilibrium models such as MINEQL+ (Schecher and McAvoy 1998) and thermodynamic data shown below in Table 1 (adapted from Grenthe et al. 1992), uranyl hydroxyl, carbonate, and hydroxy-carbonate complexes have been determined to be of most interest in aqueous environments.

Table 1. Thermodynamic Data for U Speciation with corresponding Log K values (Grenthe et al. 1992)

CHEMICAL EQUILIBRIUM EQUATIONS	LOG K VALUE
$UO_2^{2+} + H_2O \Leftrightarrow UO_2(OH)^+ + H^+$	- 5.20
$UO_2^{2+} + 2\,H_2O \Leftrightarrow UO_2(OH)_2\,(aq) + 2\,H^+$	- 10.30
$UO_2^{2+} + 3\,H_2O \Leftrightarrow UO_2(OH)_3^- + 3\,H^+$	- 19.20
$UO_2^{2+} + 4\,H_2O \Leftrightarrow UO_2(OH)_4^{2-} + 4\,H^+$	- 33.00
$2\,UO_2^{2+} + H_2O \Leftrightarrow (UO_2)_2OH^{3+} + H^+$	- 2.70
$2\,UO_2^{2+} + 2\,H_2O \Leftrightarrow (UO_2)_2(OH)_2^{2+} + 2\,H^+$	- 5.62
$3\,UO_2^{2+} + 4\,H_2O \Leftrightarrow (UO_2)_3(OH)_4^{2+} + 4\,H^+$	- 11.90
$3\,UO_2^{2+} + 5\,H_2O \Leftrightarrow (UO_2)_3(OH)_5^+ + 5\,H^+$	- 15.55
$3\,UO_2^{2+} + 7\,H_2O \Leftrightarrow (UO_2)_3(OH)_7^- + 7\,H^+$	- 31.00
$4\,UO_2^{2+} + 7\,H_2O \Leftrightarrow (UO_2)_4(OH)_7^+ + 7\,H^+$	- 21.90
$UO_2^{2+} + SO_4^{2-} \Leftrightarrow UO_2SO_4\,(aq)$	+ 3.15
$UO_2^{2+} + 2\,SO_4^{2-} \Leftrightarrow UO_2(SO_4)_2^{2-}\,(aq)$	+ 4.14
$UO_2^{2+} + CO_3^{2-} \Leftrightarrow UO_2CO_3\,(aq)$	+ 9.68
$UO_2^{2+} + 2\,CO_3^{2-} \Leftrightarrow UO_2(CO_3)_2^{2-}$	+16.94
$UO_2^{2+} + 3\,CO_3^{2-} \Leftrightarrow UO_2(CO_3)_3^{4-}$	+21.60
$3\,UO_2^{2+} + 6\,CO_3^{2-} \Leftrightarrow (UO_2)_3(CO_3)_6^{6-}$	+54.00
$2\,UO_2^{2+} + CO_3^{2-} + 3\,H_2O \Leftrightarrow (UO_2)_2CO_3(OH)_3^- + 3\,H^+$	- 0.85
$UO_2^{2+} + 3CO_3^{2-} + 2Ca^{2+} \Leftrightarrow Ca_2UO_2(CO_3)_3\,(aq)$	+29.22
$UO_2^{2+} + Si(OH)_4 \Leftrightarrow UO_2H_3SiO_4^+ + H^+$	- 1.98

2.1.1. Effects of pH and Inorganic Carbon

Using the thermodynamic data available (Table 1), and the subsurface aqueous chemical conditions, MINEQL+ (Schecher and McAvoy 1998) has been used in many instances to determine which U species are being formed in various environments. Hsi and Langmuir (1985) studied the effects of pH and carbonate complexation on the adsorption of U species to four different ferric oxide or oxyhydroxide soils. They found that, as the pH increased, the amount of U adsorption to the sediment increased in all studies, with the most adsorption occurring on the amorphous ferric oxyhydroxide suspensions. They also determined that carbonate complexation inhibited the adsorption of U onto the sediments in all studies, and that inhibition was proportional to the total carbonate concentration in solution. In comparing the various data gathered in their research, they determined that uranyl hydroxyl complexes were strongly adsorbed in relation to the weakly adsorbed uranyl carbonate and hydroxyl-carbonate complexes.

The effects of pH and dissolved carbonate concentration on adsorption have been consistent in most literature. Waite et al. (1994) analyzed the effects of U adsorption onto ferrihydrite, varying pH, CO_2 partial pressures, and U concentrations. They found that by increasing the partial pressure of CO_2 to 1%, U(VI) adsorption between pH 7 and 9 significantly decreased. They attributed this effect to the competition between iron and carbonate for uranyl complexation. This trend was seen in other research (e.g., Gabriel et al. 1998), all leading to the conclusion that by increasing the carbonate concentration, adsorption decreases due to competition between solid phase iron and aqueous phase carbonate. Interestingly, Barnett et al. (2002) found that this sharp decrease in adsorption reversed again after pH 9.5, and the amount of adsorption began to increase again. They attributed this to the inability of dissolved carbonate to compete with the increasingly negative surface charge of iron oxide for U complexation.

2.1.2. Surface Complexation

As stated previously, U reacts with a number of elements and chemical complexes, including many solids. U(VI) has been found to adsorb strongly to iron and silicate

mineral phases. Iron surface sites, both strong and weak, tend to more strongly adsorb U than other mineral phases. Silicate, which is usually found in low concentrations in sediments such as clay, does adsorb U but does not have as significant of an effect as iron. Soil calcium carbonate, on the other hand, tends to reduce the amount of adsorption occurring in the pH range of 7 to 9 (Zheng et al. 2003), so long as it is present and of significant concentration.

Iron minerals are the major focus when examining U(VI) adsorption. In the presence of iron minerals, and depending on the pH and inorganic carbon concentration, the U-solid surface complexes can be determined by a variety of existing models. The amount of adsorption onto iron sites does depend on the number of sites; the more sites that are available, the more adsorption will take place. Uranium adsorption onto iron sites is reversible. The rate of the adsorption-desorption reaction depends not only on pH, but other factors such as inorganic carbon concentration and the number of available mineral surface sites available. Studies have been conducted to determine which species adsorb to iron minerals, and which are most dominant under varying conditions, as described below.

Hsi and Langmuir (1985) suggested a number of surface complexes that could react with iron mineral (FeOH) surface sites. Included in this list are UO_2^{2+}, UO_2OH^+, $(UO_2)_3(OH)_5^+$, $UO_2(CO_3)_2^{2-}$, and $UO_2(CO_3)_3^{4-}$. They found the best fit to their data using a monodentate UO_2OH^+ complex and a bi- or tridentate $(UO_2)_3(OH)_5^+$ complex. This suggested that the $(UO_2)_3(OH)_5^+$ complex bonds to either two or three different FeO^- surface sites, with them favoring the bidentate due to the increased difficulty to find three surface sites close enough together for the U species to bond to over two.

Waite et al. (1994) contradicted the importance of the $UO_2(CO_3)_2^{2-}$ and $UO_2(CO_3)_3^{4-}$ species. They stated that when those species are dominant, there is a sharp decrease in the amount of U(VI) adsorption, thus leading them to believe that those species would not adsorb strongly to the iron surfaces. Instead, they suggested an inner-sphere, bidentate UO_2^{2+} surface complex, and a $UO_2CO_3^0$ ternary surface complex. A two-site, two-species, diffuse double-layer model fit their data accurately.

Other research has been conducted to determine which solid U complexes are formed. Bargar et al. (1999) and Wazne et al. (2003) both suggest UO_2^{2+}, UO_2CO_3, and $UO_2(CO_3)_2^{2-}$ are the important species present in the pH range above 3. Their model suggests the important complex varies as conditions change and pH increases. Overall, most studies have found that important species are dependent on the experimental conditions. Through the use of varying techniques, including X-ray adsorption spectrometry, electrophoretic mobility measurements, Fourier transform infrared spectroscopy, and Zeta potential measurements, many combinations of surface structures have been determined (Waite et al. 1994; Bargar et al. 1999; Bargar et al. 2000; Moyes et al. 2000; Bostick et al. 2002; Kelly et al. 2003; Wazne et al. 2003).

2.2. Lab Studies

Both batch and column studies have been performed on various sediments in laboratory environments to determine the effects of varying conditions on U kinetics and transport. In lab environments, the conditions of each experiment can be equilibrated in order to determine the effects of each variable on the resultant data. These effects can then be used to determine which factors have the greatest effect on the mobility or adsorption of U. With this information, models can be created to fit the data. With an adequate model, field studies can then be performed to determine potential remediation methods for contaminated sites.

2.2.1. Batch Studies

Batch experiments are done in open or closed systems under equilibrium conditions over the course of the experiment. Results include both aqueous and adsorbed data over the course of the experiment. The pH, inorganic carbon concentration or partial pressure of CO_2, anions, cations, and potentially mineral phases present can be measured. With this data, an idea of the amount of retardation and adsorption capacity of the sediment can be determined for the chosen set of experimental parameters, as well as an

idea of which complexes are formed and which are most dominant under set experimental conditions.

Most batch experiments are conducted using very small total volumes, with less than 5 grams of sediment being equilibrated to the appropriate pH, ionic strength, and carbon concentration. Barnett et al. (2000) and Barnett et al. (2002) used centrifuge tubes with 0.1 g soil to 30 ml solution, Moyes et al. (2000) had 0.1 or 0.3 grams soil to 10 or 30 ml solution respectively, where higher soil to solution volumes were used by Gabriel et al. (1998) (0.2 g/ml), and by Gamerdinger et al. (2001) (0.375 g/ml). With these small volumes, preequilibration took only a day or two unless large adjustments in pH or carbon concentration were made. With larger adjustments, equilibrium took several days to accomplish. Once the solutions were stabilized for 24 hours, in most cases acidic U solution was added and the pH was readjusted back to the appropriate value using NaOH (the exception being Gamerdinger et al. [2001], who added U in the form of Uranium Nitrate Hexahydrate [$UO_2(NO_3)_2*6H_2O$] to Hanford groundwater to make their five U solutions of varying concentrations, and then added this to their preequilibrated sediment).

Uranium experiments were allowed to equilibrate for anywhere between 24 hours (Moyes et al., 2000) to 12 days (Gabriel et al., 1998). Once equilibration had been obtained, the samples were centrifuged to separate solid and aqueous phases, and the aqueous phase filtered prior to analyses. Uranium was analyzed through the use of Kinetic Phosphorescence Analyzers (KPA) (Waite et al. 1994; Barnett et al. 2000; Barnett et al. 2002), Inductively Coupled Plasma-Mass Spectrometry (ICP-MS) (Moyes et al. 2000; Gamerdinger et al. 2001), or Time-Resolved Laser-Induced Fluorescence (TRLIF) Spectroscopy (Gabriel et al. 1998).

Many determinations have been made from previous experimental data. Waite et al. (1994) determined a slight dependence of adsorption to ionic strength occurred for alkaline solutions. They also determined there was an increase in the amount of adsorption with an increase in the amount of available ferrihydrite. Their resultant nonlinear adsorption trend was fit using the Freundlich isotherm. They also found a best fit to their data using a two-site, two-species model, suggesting that both strong and weak iron adsorption sites were present and that both UO_2^{2+} and $UO_2CO_3^0$ surface complexes

were responsible for the adsorption of U onto their sediment. Barnett et al. (2000) also found that as ionic strength increased from 0.01 to 0.1M in their study, the amount of U adsorption decreased. This was attributed to competition for adsorption sites by the sodium counter-ion in their background electrolyte, suggesting adsorption may be attributed to reversible outer-sphere surface complex formations. They fit their data using Freundlich isotherms, and attributed the need for this model to the adsorption of U to different types of surface sites as a function of surface loading.

Barnett et al. (2002) analyzed potential species formation and the reasoning behind the observed trend of percent adsorption vs. pH for their batch experiments. They attributed the increase in adsorption from pH 4 to 5 as a decrease in the aqueous UO_2^{2+} and an increase in adsorbed UO_2^{2+}. Between pH 5.5 and 8, the dominant adsorbed species was hypothesized to have switched from UO_2^{2+} to adsorbed $UO_2CO_3^{0}$. Adsorption then decreased sharply between pH 8 and 9, which was attributed to the formation of $UO_2(CO_3)_3^{4-}$ (misprinted as $UO_2(CO_3)_4^{2-}$ in their article) the dominant aqueous complex under their experimental conditions. In the absence of carbonate they found a similar trend, with UO_2^{2+} as the dominant aqueous species up to pH 4.5, where it began to adsorb onto iron sites on the sediment. UO_2^{2+} was the dominant adsorbed species up to pH 9, where the subsequent formation of aqueous $UO_2(OH)_3^{-}$ began to decrease the amount of adsorption. Both experiments were done in batches with open environments, where pH and CO_2 were in equilibrium with atmospheric conditions. Systems with constant carbonate concentration were analyzed to determine if the adsorption effects changed in a closed environment. The resulting data showed a decrease in the maximum concentration of adsorbed U as well as less adsorption in the alkaline pH range. They also found that the $UO_2CO_3^{0}$ surface complex was the dominant species and adsorbed UO_2^{2+} played little role until the pH was above 9. They hypothesized this was due to the inability of the dissolved carbonate to compete with the increasingly negative surface sites for U complexation.

Overall, batch results give an idea of what could be expected to occur in subsurface environments under varying conditions. With batch experiments though, the amount of dissolved species in solution is generally much higher than it will be in

flowing systems due to the closed environment. This leads to higher ionic strengths, increased accumulation of ions that would not normally be present in a flowing environment, and the possible over- or under-predictions of what would occur in the field. It does, on the other hand, give a good starting point on what could be expected to occur with flowing systems.

2.2.2. Column Studies

Barnett et al. (2000) gave four good reasons as to why batch experiments don't necessarily apply to transport in the subsurface: 1) the solid to solution ratio is typically lower than what would be found in the subsurface, 2) there is generally a higher concentration of reaction products and intermediates than would typically occur in a flowing system, 3) hydrodynamic mass-transport limitations that would potentially occur in porous media are not accounted for, and 4) the reactivity of the mineral phases may change due to particle abrasions, etc. These observations point out the importance of column studies.

Similar to batch studies, column experiments have generally been conducted to determine the effects of varying geochemical parameters on the adsorption and transport of U. Gabriel et al. (1998) compared two columns, one packed with 100 g pure sand and the other with 100 g sand and 0.62 g goethite-coated sand, both having similar porosity and sediment volumes. They used two different flow rates (3 and 30 cm^3/hr), a carbonate concentration of 0.01 M equilibrated with atmosphere, chloride as an inert tracer, and varying U pulses of 0.05, 0.1 and 1 μM. In the column with goethite, the pH ranged from 8.85 to 9.35, and varied from 9.4 to 9.6 in the one without. They found that increasing flow resulted in breakthrough curves with similar retardations but different shapes. Equilibrium was established at the lower flow, but not at the higher. All experiments with goethite-coated sand resulted in non-symmetrical shape, indicating nonlinear adsorption. The pure sand column resulted in practically no retardation at pH 9, leading to the conclusion that there were no reactions taking place in the absence of goethite. It was also determined that adsorption reactions were reversible in all instances due to the

near complete recovery in all cases. Two sites, strong and weak, were incorporated into their surface complexation modeling, with a ratio of 1:200 respectively.

Barnett et al. (2000) used natural soils from Oak Ridge (OR), TN, Savannah River (SR), GA, and Hanford (HF), WA. No adjustments were made to the natural chemistry and pH of the sediments prior to use in the lab. Two grams of sediment were packed to a depth of 1.7 cm in a 1 cm diameter glass column for each of their three sediment types. Each used 0.01 M $NaNO_3$ as the aqueous transport solution, which was pH adjusted to the appropriate natural soil pH. The flow was set to 4.3 cm/hr, with a residence time of 0.18 hours. Once the column was saturated, a step input of U in 0.01 M $NaNO_3$ matrix was introduced for at least 23 days, and then switched back to U free 0.01 M $NaNO_3$. Samples were taken over the course of the experiment. The natural pH of the sediments were 4.1 (SR), 4.7 (OR), and 6.8 (HF). Breakthrough of U in each column took over 3000 pore volumes, with the Hanford column taking the longest (over 6000 pore volumes) before breakthrough was accomplished. All curves were asymmetric, leading to the assumption of rate-limited and/or nonlinear adsorption. Almost complete mass recovery was accomplished over the course of all experiments, indicating reversible adsorption. Adsorption was found not only to be pH dependent, but it was also suggested that the similar iron contents of these sediments strongly controlled this process.

The effects of sediment saturation were analyzed by Gamerdinger et al. (2001). They used both coarse and fine sands from Hanford, WA, as well as natural uncontaminated Hanford groundwater. Their sediments were packed in columns and saturated with Hanford groundwater. They were placed in a centrifuge to establish steady-state unsaturated flow and water content. Hanford groundwater was also used in saturated columns and equilibrated. Step inputs of approximately 500 μg/L aqueous UO_2^{2+} were added for variable numbers of pore volumes depending upon the experiment. Experimental variables included the percent saturation, the average pore water velocity, and the U step input time. They found that a two-site model fit experiments with water contents of 66% or more, whereas a two-region model fit experimental data for water contents of less that 30% saturation. At low water contents, adsorption and effective retardation were found to be significantly less than predicted from batch studies. It was

assumed that sites in the immobile water region were cut off from the flow, leading to increased U mobility. Increasing pore water velocity showed less adsorption, leading to the conclusion that adsorption was rate-limited.

2.3. Summary of Past Work

Through the research that has already been conducted, much has been learned about how U reacts in subsurface environments. Both the aqueous and surface complexes have been studied, and models have been proposed that can accurately fit experimental data. Since most subsurface environments contain carbonate and are potentially completely saturated flowing systems, the uranyl hydroxyl, carbonate, and hydroxyl-carbonate species are of most interest, with a two-site, two-species model showing the best fit to experimental data in most cases. Many surface complexes have been considered, with the UO_2^{2+} and $UO_2CO_3^0$ species being potentially of most importance in environments where iron-surface reactions are most prevalent. Waite et al. (1994) state the major differences in approaches to surface modeling are the choice of surface complexes under acidic conditions, where there is a lack of CO_3^{2-} present, and the number, potential importance, and type of uranyl-carbonate surface complexes. They also conclude through their results that the surface complexes formed are unique products of the surface environment and not of the predominant U aqueous species.

3. MATERIALS AND METHODS

3.1. Preparation of Artificial Groundwater and Tracer Solutions

Preparation of the artificial groundwater and tracer solutions were done as described below.

3.1.1. Hanford Artificial Groundwater

An artificial groundwater recipe for the Hanford site was obtained from Dr. Jim Szecsody at Pacific Northwest National Labs in Richland, WA. With the use of MINEQL+ version 4.0 (Schecher and McAvoy 1998) and testing in the lab, the recipe was modified to ensure proper concentration of species and no precipitate formation under experimental conditions. This entailed removing calcium and magnesium salts from the groundwater recipe and replacing with their sodium salt counterparts.

In order to run varying carbonate and pH to determine their effects on U transport, the carbonate concentration and amount of acid or base added was modified for each experiment. Sodium bicarbonate was added at values of 84 and 841 mg/L to reach carbonate concentrations of 1 mM and 10 mM respectively. To reach the desired pH for the experiment, 1 M HNO_3 or NaOH was used. Synthetic uncontaminated Hanford groundwater recipes for 1 and 10 mM inorganic carbon can be found in Appendix I.

The uncontaminated Hanford artificial groundwater solutions were prepared 20 liters at a time and kept in gas tight tedlar bags to ensure no loss of CO_2. All artificial groundwater was prepared using DI. It was mixed in a 20 liter glass using a magnetic stirrer until all solids were dissolved before transfer via pump into closed bags.

3.1.2. Uranium/Bromide Tracer Solution

The U/Br tracer was prepared as a ten times concentrated solution. Uranium stock solution was made by dissolving Uranyl Nitrate-Hexahydrate crystals in 0.1 M HNO_3 to obtain a 1 liter volume of 1000 ppm U in solution. The tracer solution was then made

using 50 mL U stock solution to 450 mL artificial groundwater. 44.7 mg Br, in the form of Potassium Bromide, was also added to this solution as a non-reactive tracer. The pH was adjusted to match that of the experimental conditions by using either 1 M NaOH or HNO_3. Synthetic Hanford groundwater recipes with U/Br tracer for 1 and 10 mM inorganic carbon can be found in Appendix II.

3.2. Experimental Design

In analyzing experimental results from the literature, it was decided that a series of experiments would be done to determine the impact of different chemical variables on the transport of U species through Hanford sediment. In experimenting with the transport of U through the sediment, there were two main variables that would be analyzed: pH and inorganic carbonate concentration. Table 2 was developed to outline how the experiments would be carried out. Each experiment would vary only one parameter, so as to easily determine the impact of the specific changes.

Table 2. Experimental Plan for U Transport Analysis

Experiment #	1	2	3	4
Criteria				
pH	9	9	6.5	4
CO_3^- (mmol/L)	10	1	10	10
Q (mL/min)	2.5	2.5	2.5	2.5
UO_2^{2+} (mg/L)	1	1	1	10

3.3. Experimental Methods

Solubility tests, batch isotherm experiments, and column experiments were conducted in this research. Solubility tests were used to determine the maximum concentration of U that could be dissolved in the groundwater solution without precipitation. Batch isotherm experiments were done at U concentrations from 1 to 200 mg/L for pH 4, 1 to 75 mg/L for pH 6.5, and 1 to 50 mg/L for pH 9 to get a preliminary idea of how U would adsorb to sediments under the different aqueous conditions.

Breakthrough curves and analysis of the effects of pH and inorganic carbon concentration on the flow of U were determined from the column experiments.

3.3.1. Solubility Test

Solubility tests were performed as a first step to determine the maximum concentration of U that would completely dissolve in the specified Hanford groundwater solution for the upcoming column experiment. Groundwater was made at the specified pH and inorganic carbon concentration for the experiment as described above, and 90 ml were transferred to a clean beaker. 1000 ppm U stock was then added and pH adjusted using 1 M NaOH as necessary. Total volumes of U stock and NaOH were recorded until U salts precipitated out of solution (determined on the basis of color and overnight settling). The concentration of U in solution without causing precipitation was calculated based on the total volume of U added and the aqueous volume, and subsequently double checked by filtering the solution using 0.2 μm syringe filters and analysis with a KPA. This value was used as a maximum concentration that could be used in batch and column studies.

3.3.2. Batch Experiments

Batch experiments were conducted using 250 ml I-Chem Boston round bottles with open-top 0.125 inch septa caps. New bottles and caps were weighed and the weights recorded. Approximately 200 grams wet Hanford sediment, which had been saturated with synthetic Hanford groundwater at the necessary pH and inorganic carbon concentration, was added to the bottles. The weights were again measured and recorded. The bottles were then filled with the proper amount of synthetic groundwater, weighed and recorded, and placed on a horizontal roller overnight.

The next day, 6 ml samples were taken from each bottle using a syringe, and the sample volume was replaced with synthetic groundwater. The sample was analyzed for pH and the value recorded. Small volumes of 1 M HNO_3 or NaOH were added to alter

the pH if necessary, and added volumes of acid or base were recorded. The bottles were again placed on the roller for at least 12 hours and the process was repeated until the pH had equilibrated (established as giving constant results over a 24 hour period). The bottles were then checked for inorganic carbon concentration by taking 4 ml samples from the bottles, filtering using 0.2 μm syringe filters into 2 ml sample vials, and analyzing using a TOC analyzer. Increasing inorganic carbon concentration was done by replacing calculated volumes of supernatant with synthetic groundwater at the appropriate pH but higher inorganic carbon into the bottles, while reduction of the inorganic carbon concentration was done by sparging with N_2 gas. If the inorganic carbon was reduced, pH and inorganic carbon were rechecked and adjusted separately until the appropriate values were achieved. In general, sample equilibration took days or weeks to achieve.

3.3.2.1.Batch Isotherm Experiments

In order to determine how U adsorbs to Hanford sediment at each pH and inorganic carbon concentration, batch experiments were conducted under the pH and inorganic carbon conditions indicated in Table 2. Using data obtained from solubility tests, appropriate volumes of U solutions were made for injections to the bottles. A total of twelve bottles were assembled and analyzed for each experiment. Uranium concentrations were run in duplicate, as well as a blank with sediment and a control containing 10 ppm U and no sediment. Dry bottle weights (with lid), bottle weights with addition of wetted sediment, and bottle weights with sediment and groundwater were recorded prior to running the experiments.

Appropriate volumes of U injection solution, previously adjusted to the appropriate pH for the experiment, were prepared as described above and transferred to various syringes for injection to reach the desired aqueous U concentrations into the appropriate labeled bottle. The volume of injection solution added was calculated on the basis of total volume of groundwater in each bottle, the injection solution concentration, and the desired U concentration for each bottle. After injection of U, the bottles were

mixed by manually rotating them vertically 180 degrees three to four times to ensure sediment and aqueous phase mixing, and a 4 ml sample was taken at time t_o. The bottles were then placed on a horizontal roller and allowed to mix. Sample times were 0, 5, 10, 20, 60, 120, 240, 480, and 960 minutes. Each sample was taken via syringe and transferred through a 0.2 μm syringe filter into 2ml sample vials, and then immediately closed using a septa screw top lid.

At the conclusion of the experiment, the samples were analyzed for inorganic carbon and U, using a TOC analyzer and a KPA analyzer respectively. Filtered samples were also taken from each of the batch bottles containing both U and sediment after all analyses were done and analyzed for anions and cations using Ion Chromatography (IC) and Inductively Coupled Plasma (ICP) to determine the ionic strength and ion concentrations of each bottle (see Appendix IV). The bottles were dried over a period of 48 hours in a 125°C oven. Once completely dry the bottles were weighed. With the dry weight of the bottles and sediment, accurate calculations on sediment and groundwater volumes could be done allowing for more precise determinations of actual initial aqueous U concentrations.

3.3.3. Column Experiments

All experiments were conducted using the same column setup (Figure 1). The inlet of the column consisted of a 1 liter stainless steel ISCO Model 500D dual syringe pump with an ISCO Series D pump controller for injection of uncontaminated synthetic groundwater. A 50 ml Gilson 402 dual syringe pump with two 25 ml Gilson glass syringes was used for injection of the tracer solution, with a three-way stainless steel valve connecting the two pump outlets for mixing the two solutions. The column was made of stainless steel, 50 cm long and 5 cm in diameter. A Gilson 223 Sample changer, using 735 Sample Software, was in line with the outlet of the column for taking samples at selected time intervals throughout the experiment. Waste containers collected the remaining aqueous flow out of column.

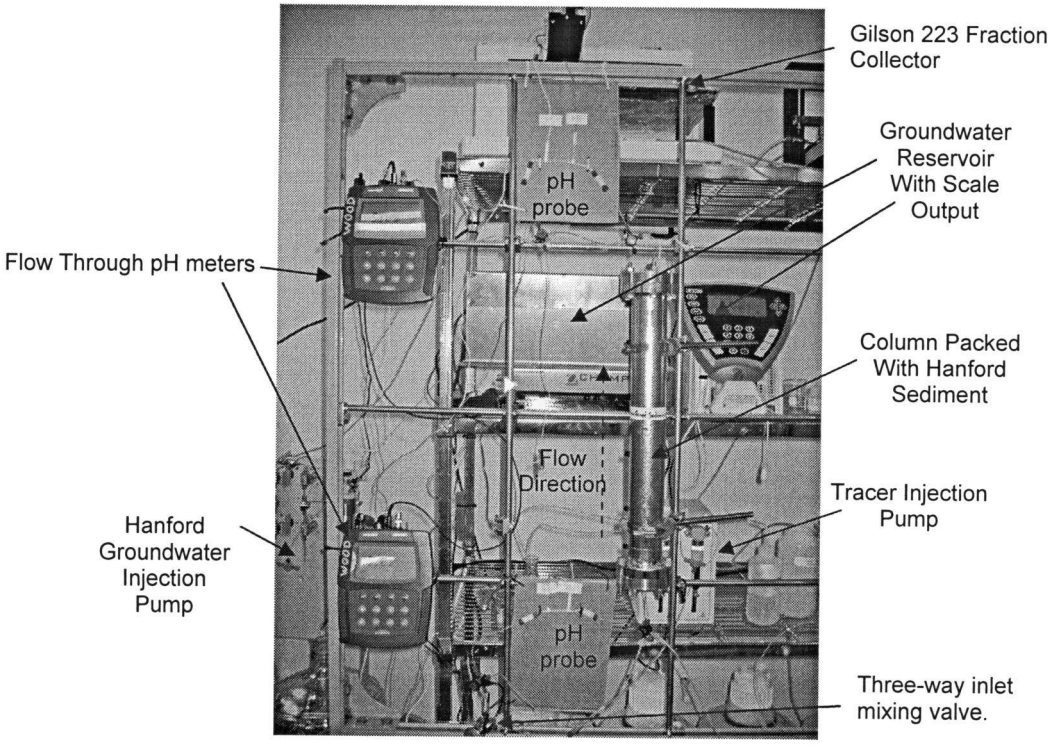

Figure 1: Column setup. Included is the influent groundwater reservoir, inlet pump, tracer pump, column packed with Hanford sediment, fraction collector, and flow through pH probes and meters.

3.3.3.1.Hanford Sediment Description

Hanford sediment was obtained through Dr. Jack Istok at Oregon State University, who obtained the sediment from a quarry at the Hanford formation near Pasco, WA. It consists of sands and gravels, with less than 5% silt and clay. Iron made up approximately 6 wt %, with the available iron being only 0.15 wt % of the total mass. Sediment was collected from Dr. Istok, and sifted through a No.4 screen (4.76 cm opening) to ensure all large particles were removed.

3.3.3.2.Column Packing Procedure

Sediment was placed in the column using a wet packing method. For the half-meter stainless steel column, one end was assembled by placing the frits, o-rings, and cap in place, and fastening them with six ½" bolts. Tubing (1/8" PEEK and 1/16" stainless steel) was attached to this end with a valve to open or close the line, and a luer lock fitting was used to inject groundwater from the bottom of the column.

Using a syringe, approximately 20 ml groundwater was injected into the column from the bottom, and then enough sediment was added from the top to fill just above the liquid level. A rubber mallet was used to tamp the side of the column, ensuring the sediment was packed tightly below liquid level and all trapped air was removed. The volumes of sediment and groundwater were measured using a scale and recorded. This process was repeated until the column was packed to the point where the screens were to be placed at the top.

The top screens, o-rings, and lid were put in place and then secured using six ½" bolts. Tubing (1/16" PEEK) was attached to the top of the column and the unit was secured in place for use. The column inlet was then set in line with the ISCO syringe pump, and the outlet connected to the Gilson sample changer. The column was flushed with synthetic Hanford groundwater until the pH and inorganic carbon concentration reached equilibrium at the appropriate levels for each experiment.

3.3.3.3.Column Experiments

Column experiments were run at the pH and inorganic carbon concentrations identified in Table 2. As can be seen in the schematic of the column setup (Figure 1), a solution containing U and Br tracer, which was 10 times concentrated, was pumped through the inlet mixing valve at a flow rate of 0.25 ml/min, with Hanford groundwater being injected through the same valve at 2.25 ml/min. The total flow rate through the column resulted in one pore volume taking 150 minutes. The tracer was injected for one pore volume, then the tracer pump was stopped and uncontaminated groundwater flow was increased to account for the loss. Samples were taken at constant time intervals using a Gilson 223 fraction collector. Each rack of samples for the fraction collector holds 96 samples. After the last sample in a rack was taken, the rack was replaced and the sampling reinitiated if necessary. The software was then restarted if changes were made, and samples were collected as specified.

Bromide concentration was determined using IC, while U was analyzed using a KPA. Inorganic carbon and pH were also checked periodically from the column influent and effluent to ensure equilibrium of these parameters.

3.4. Modeling

Three programs were used to model the results of each experiment. Aqueous speciation and chemical equilibrium were modeled using MINEQL+ (Schecher and McAvoy 1998). This program used pH, ion concentrations (see Appendix V), and component data to determine how aqueous species were distributed for each experiment. Aqueous and adsorbed speciation was modeled together using FITEQL (Herbelin and Westall 1999). This model incorporated the adsorption of U to iron sites, which could not be adequately modeled with MINEQL+. Modeling of the resultant Br and U breakthrough curves were accomplished using the transport code CXTFIT version 2.1 (Toride et al. 1999). This program was used to fit the experimental breakthrough curve data and estimate values for transport and reaction parameters.

3.4.1. MINEQL+, version 4.0 (Schecher and McAvoy 1998)

The chemical equilibrium modeling software MINEQL+ calculated % Total U vs. pH diagrams for each column experiment. This showed dominant aqueous U species present under the conditions for each set of experimental parameters. To run the simulation, ion concentration data determined from each experiment was input into the program (see Appendix V), pH and inorganic carbon concentrations, set as a closed system, were fixed, the ionic strength was set to be calculated, and the titration simulation was run with the resultant data being transferred to excel for visual interpretation.

3.4.2. FITEQL, version 4.0 (Herbelin and Westall 1999)

The computer program FITEQL was used to produce surface speciation diagrams using information for aqueous speciation from Grenthe et al. (1992), and surface complexation information from Waite et al. (1994). Surface site concentration was calculated from experimental data, with concentrations for strong and weak surface sites of 0.8732 moles sites/mole Fe and 0.0018 moles sites/mole Fe (Waite et al. 1994) respectively. Ionic strength (calculated from MINEQL+), pH, and inorganic carbon concentrations were all fixed as a closed system and the speciation diagrams were produced from the resultant output file using excel.

3.4.3. CXTFIT version 2.1 (Toride et al. 1999)

The transport code CXTFIT can be used either for estimating transport parameters from observed data (using inverse fitting) or predicting concentrations for specified parameter sets. For this research, the inverse fitting was done to estimate parameters for both Br and U breakthrough curves for all column studies. Bromide was used as a non-reactive conservative tracer. All Br data was fit using the deterministic equilibrium model. Both a two-region and a two-site model have been suggested to fit U data. For this research, the deterministic two-site nonequilibrium model was used.

All parameters were kept in dimensional form, using flux-averaged concentrations in all cases. Constraints of D and v were used for estimation of fitted parameters for U data only, and total mass was not estimated for Br or U. Both elements were single pulse inputs with 150 minute durations. Units for Br were cm, min, and mg, while U data was in units of cm, min, and nanograms.

3.4.3.1.Deterministic Equilibrium CDE

The deterministic equilibrium CDE is used for one-dimensional transport of solutes in homogeneous soils. It is assumed that Br undergoes steady-state transport, and there is no adsorption, degradation, or production taking place. This leads to the following general equation:

$$R\frac{\partial c_r}{\partial t} = D\frac{\partial^2 c_r}{\partial x^2} - v\frac{\partial c_r}{\partial x} \tag{1}$$

R, known as the retardation factor, is given by:

$$R = 1 + \frac{\rho_b K_d}{\theta} \tag{2}$$

Here, D is the dispersion coefficient (cm^2/min), v is the pore-water velocity (cm/min), ρ_b is the bulk density of the sediment (mg/cm^3), K_d is the empirical distribution constant (cm^3/mg), θ is the porosity (cm^3/cm^3), and c_r is the resident concentration in the aqueous phase (mg/cm^3).

In fitting of the breakthrough data, it was assumed that R was equal to 1 in all cases. Initial injection concentrations were determined by mass balance of breakthrough curve data to allow for a better fit with this program. ρ_b for the column was 1844.66 mg/cm^3, and θ was determined to be 0.38. These values were calculated for this column prior to running any experiments. CXTFIT was used to determine values for D and v, which were then used in fitting U data from the same experiment.

3.4.3.2.Deterministic Two-Site Nonequilibrium CDE

Due to the abundant tailing seen in three of the four U breakthrough curves, it was assumed that there were either physical and/or chemical kinetics causing nonequilibrium transport. Physical nonequilibrium is modeled as if there are both stagnant and flowing regions throughout the column interacting through first-order kinetics; whereas chemical nonequilibrium is modeled as though there are two distinct types of adsorptive sites, one at equilibrium and the other governed by first-order kinetics. It was assumed that the column was completely saturated, and that there were no stagnant regions or diffusion limitations in these experiments. Uranium was modeled using the two-site nonequilibrium CDE. It was assumed that no production or decay of U occurred throughout the experiment, thus the values of μ and γ were taken as zero, leaving the following:

$$\left[1+\frac{f\rho_b K_d}{\theta}\right]\frac{\partial c}{\partial t}=D\frac{\partial^2 c}{\partial x^2}-v\frac{\partial c}{\partial x}-\frac{\alpha\rho_b}{\theta}\left[(1-f)K_d c-s_k\right] \tag{3}$$

$$\frac{\partial s_k}{\partial t}=\alpha\left[(1-f)K_d c-s_k\right] \tag{4}$$

In these equations, f is the fraction of exchange sites that are always at equilibrium, α is a first-order kinetic rate coefficient (1/min), and s_k is the kinetically controlled surface concentration. First order adsorption and desorption rate constants can also be determined from the previous equations by:

$$k_1=\alpha(1-f)K_d \tag{5}$$

$$k_{-1}=\alpha \tag{6}$$

The values for v and D from the Br curve were utilized in the fitting of the U using the deterministic two-site nonequilibrium model in CXTFIT. This yielded values for R, β (dimensionless partitioning coefficient), and ω (dimensionless mass transfer coefficient).

3.5. Analytical Methods for Sample Analysis

Uranium, bromide, inorganic carbon, and pH were analyzed in all experiments. Uranium concentrations were obtained using a Chemcheck KPA-11 Kinetic Phosphorescence Analyzer (KPA), located in the Oak Creek Building at Oregon State University. Bromide was analyzed with a Dionex DX-120 Ion Chromatograph (IC) with a Dionex AS40 Automated Sampler, also located at the Oak Creek building. Inorganic Carbon analysis was done using a Rosemount Analytical Inc. Dohrmann Division DC-109 High Temperature Total Organic Carbon (TOC) Analyzer, located in the Merryfield Lab. The VWR SR601C Symphony pH/ISE/Cond meter with VWR 14002-778 Ag/AgCl pH, Gel & 3-in-1 Symphony electrode, Microelectrodes MI-411 Combination pH needle electrode, and Microelectrodes 16-705 Flow-Thru pH electrode with 16-702 Flow-Thru reference probes in Merryfield Lab 104G were used to determine pH.

3.5.1. Kinetic Phosphorescence Analyzer – U Analysis

The KPA relates the intensity of a beam of light reflected through a glass sample cuvette to the total concentration of U in the sample. A pulsed dye nitrogen laser beam passes through the reference cell prior to the sample cell during analysis. The reference cell is used as a standard in normalizing measurements of the sample, and corrects for instrument fluctuations, including laser brightness and temperature changes. Sensitivity is optimized using mirrors, lenses and high performance interference filters. The lenses can get dusty if the sample door is left open, and should be checked and cleaned if necessary by removing the dust. The KPA counts the number of photons of photoluminescence between each laser pulse as a function of time. Measurements for intensity are taken at fixed intervals in time, known as time gates, following each laser pulse and summed over the number of pulses used in each measurement. For U, time gates 5 through 49 are used, each being 13 μs in length, and a total of 1000 laser pulses are used. This eliminates most short-lived luminescence sources and provides considerable amounts of data for calculating precise results with adequate data processing time. The analytical range is over 1,000,000, with detection limits from 0.01 to 50,000

ppb using both low and high calibration options. Low calibration reads linearly between 0 and 20 μg/L, while high calibration is used for the concentrations up to 5 mg/L.

In using the KPA for this research, all samples are diluted 1:100 using a Hamilton Micro lab 500 series Auto diluter with one 1000 μl and one 50 μl glass syringe. The auto diluter aspirates 10 μl of the sample into the 50 μl syringe, 990 μl of 0.1 M HNO_3 into the 1000 μl syringe, then dispenses both solutions into the glass cuvette. 1.5 ml Uraplex solution, used as a complexation agent for U analysis, is added to the cuvette; the sample is capped, manually mixed, all four sides wiped clean thoroughly, and then placed in the KPA for analysis. A background sample was used to determine the intensity of the groundwater without any U addition. Background intensities should be in the range of a few hundred counts, usually between 300 and 600. This value is subtracted from all subsequent samples in the software, thus it is important to have a clean, accurate background reading.

Standards were made for U with concentrations of 10, 100, 250, 500, 1000, and 2500 micrograms per liter to calibrate the machine and create a standard curve of intensity vs. U concentration in μg/L. The KPA has the option of calibration in both a low and high concentration range. For simplicity, only the low range was used, with samples outside this range diluted using the auto diluter to be within this range. The typical calibration of the standards should look similar to that in Table 3:

Table 3. Uranium standard concentrations (μg/L) and their corresponding intensity values for a low range calibration of the KPA.

Standard	Intensity
10 μg/L	502
100 μg/L	6358
250 μg/L	15457
500 μg/L	32153
1000 μg/L	69529
2500 μg/L	156942

Once background and standards were analyzed, samples could be analyzed for U. All R^2 values should be above 0.99 and lifetimes should be above 250 for the reference, standards, background, and samples. This indicates that the machine is working properly. If the values are lower, the reference should be replaced with new solution. As maintenance, reference solution in the cell should be replaced once every two weeks, and the dye (Stilbene-420) replaced every two to three months. As the laser power in the analyzer begins to degrade, the intensity readings will begin to decrease, but calibration will still be linear. The nitrogen laser plasma cartridge should be replaced once per year or at $2x10^7$ pulses, whichever comes first. Some elements have been found to interfere with the accuracy of the KPA's detection capability for U. These are detailed in Appendix III.

3.5.2. Ion Chromatograph – Bromide Analysis

Bromide was injected into each column experiment as a conservative tracer, with an inlet concentration of 30 ppm. Concentrations in the effluent samples were measured using an IC to show the column was working effectively and there were no problems with the U tracer injection. Due to high nitrate concentrations in the groundwater, IC analysis was done at the Oak Creek building at OSU by Mr. Jesse Jones (Faculty Research Assistant). The IC was set up to separate bromide and nitrate peaks using a column with a longer retention time. In order to run the IC, standards were made at concentrations of 5, 25, 50, 75, and 100 ppm of not only bromide, but chloride, nitrate, nitrite, and sulfate as well.

0.6 mL of the standards, the first four pore volumes of the experiment, two initial samples of 1:10 diluted tracer water entering the column, and an injection sample were transferred to 0.5 ml IC poly vials using an auto pipette. The samples were then sealed with filter caps pushed in until flush with the top of the vial and placed in racks. The racks were then placed in the auto sampler for the unit. The carbonate eluent was replaced in the machine, the nitrogen gas was turned on at the tank, and the program method and schedule were created on the computer system attached to the machine.

Once everything was set up and equilibrated, the computer was set to run and the samples were analyzed. Concentrations were determined automatically by the IC software, through linear calibration of peak area to standard concentrations.

3.5.3. TOC Analyzer – Inorganic Carbon Analysis

In order to determine the inorganic carbon levels flowing through the column were in the correct range, a DC-109 High-Temperature TOC analyzer was used. This gave readings for total carbon, inorganic carbon, and/or total organic carbon in units of mg/L as carbon. Three TOC standards were made by diluting a 10,000 ppm organic carbon stock made using potassium acid phthalate (KHP). The standards were analyzed for TOC, and a calibration curve was made for TOC (mg/L as organic carbon) vs. analyzer values. This linear calibration was adjusted for use with IC data by replacing the intercept with that for inorganic carbon determined from DI.

Samples from each bag of groundwater to be used in the experiments, inlet and outlet samples from the column, and samples during each column experiment were analyzed to ensure the inorganic carbon concentration stayed constant throughout. Samples from batch experiments were also analyzed to ensure constant inorganic carbon concentrations.

4. RESULTS

4.1. Solubility Test Results

Total concentrations of U obtained in solution and used as injections for each of the six batch experiments are shown in Table 4 below.

Table 4. Uranium Injection Concentrations used for Batch Experiments, determined as maximum solubility points for U at the pH and inorganic carbon concentration shown.

pH	Inorganic Carbon (mM)	U Injection Concentration (µg/L)
4	10	950.00
6.5	10	387.00
9	1	212.86
9	10	238.88

4.2. Batch Experimental Results

Equilibrium aqueous vs. adsorbed concentration was graphed for each U injection concentration. Data was fit with a linear trend line as well as using the Freundlich isotherm approach. Linear adsorption showed R^2 values between 0.963 and 0.993 for aqueous U injection concentrations up to 50 ppm. The slope of this line was used to determine a K_d and retardation value using the following equations:

$$S = K_{eq} C \tag{7}$$

$$K_d = \frac{K_{eq}}{1 - f} \tag{8}$$

$$R = 1 + \frac{\rho_b K_d}{\theta} \tag{9}$$

Bulk density (ρ_b) and porosity (θ) had been calculated previously as 1844.66 g/L and 0.38 respectively. The fraction of equilibrium sites were determined from column studies

to be approximately 0.2 for all except the pH 4, 10mM Inorganic Carbon experiment, where it showed a value of 0.468. Resultant isotherms are shown in Figures 2 through 5.

Freundlich Isotherms are non-linear and are written in the form $S = K_f C^{1/n}$, or in log-log format as $Ln(S) = \left(\frac{1}{n}\right) Ln(C) + Ln(K_f)$. This method's fit can be used to justify the assumption of multiple sites responsible for U binding with the sediment. As sites with strong surface bonding energy get filled, there is a strong increase in the curve. As these sites become full, the weaker binding sites begin to fill leading to the decrease in slope and thus the non-linear shape. On a log-log plot, the curve is linear, with an intercept equal to the Freundlich adsorption coefficient, K_f, and a slope of $\frac{1}{n}$, where n is an empirical coefficient for the isotherm. Experimental data fit using the Freundlich isotherms showed R^2 values between 0.993 and 0.997. Statistically, this is a slightly improved result than that for the linear isotherm, suggesting the possible presence of multiple binding sites. Experimental data fit with the Freundlich isotherm are shown in Figures 6 through 9.

4.2.1. MINEQL+ Speciation Simulations

Speciation diagrams were created for each batch experiment, with ion concentrations measured through various analytical methods (see Appendix IV). Uranium was measured via KPA, CO_3^{2-} concentrations through TOC analysis, IC measured Cl^-, NO_3^-, and SO_4^{2-}, and Ca^{2+}, K^+, and $Si(OH)_4$ were determined with an ICP. These values were input into MINEQL+ with the appropriate pH and U speciation data from Grenthe et al (1992). Ionic strength, charge balance, aqueous U complexes, and total dissolved concentrations were calculated. Aqueous speciation diagrams of percent total U vs. pH are shown in Figures 10 through 13.

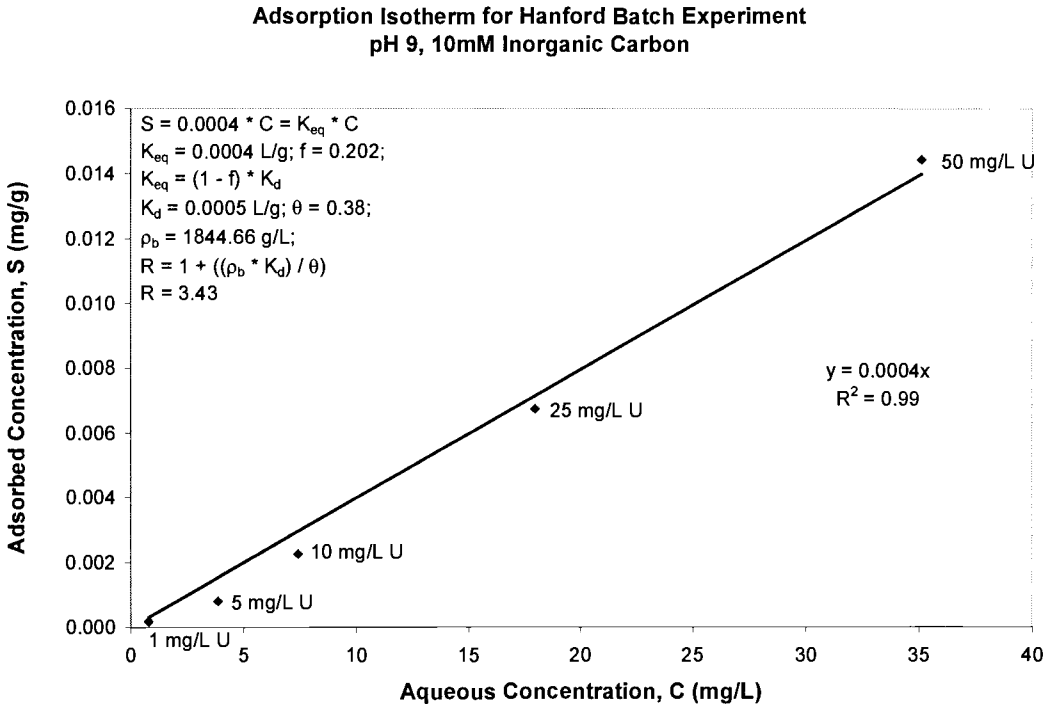

Figure 2: Adsorbed vs. aqueous U concentration for pH 9, 10 mM inorganic carbon Hanford batch experiment. Aqueous U is between 1 and 50 ppm, with 0.8 g/ml solid to solution ratio.

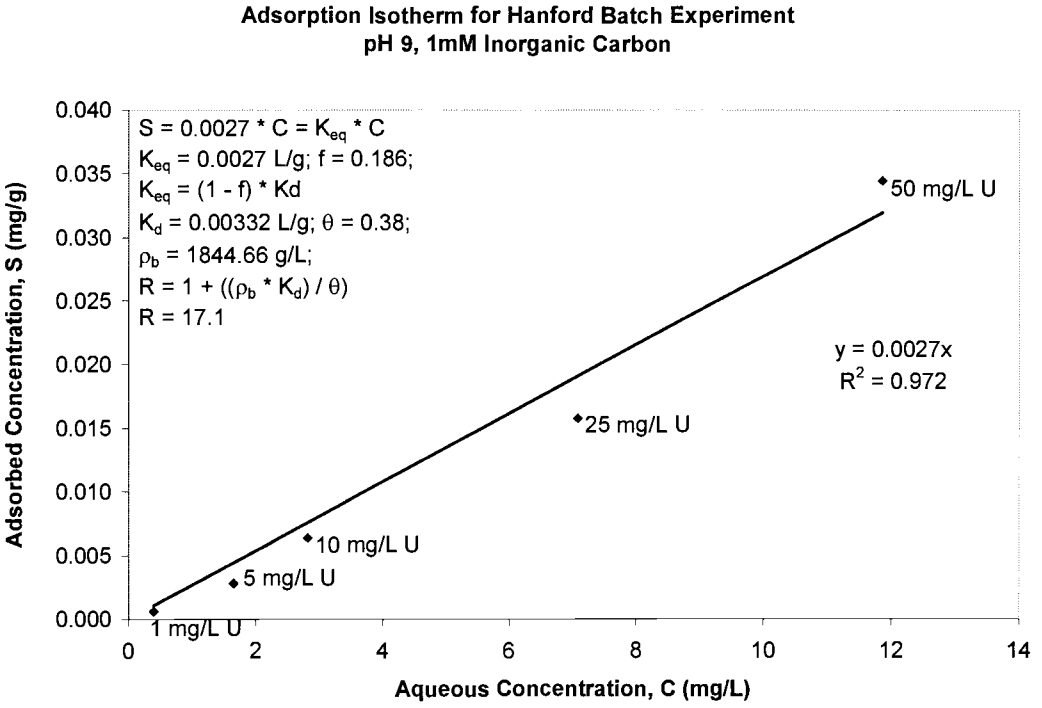

Figure 3: Adsorbed vs. aqueous U concentration for pH 9, 1 mM inorganic carbon Hanford batch experiment. Aqueous U is between 1 and 50 ppm, with 0.8 g/ml solid to solution ratio.

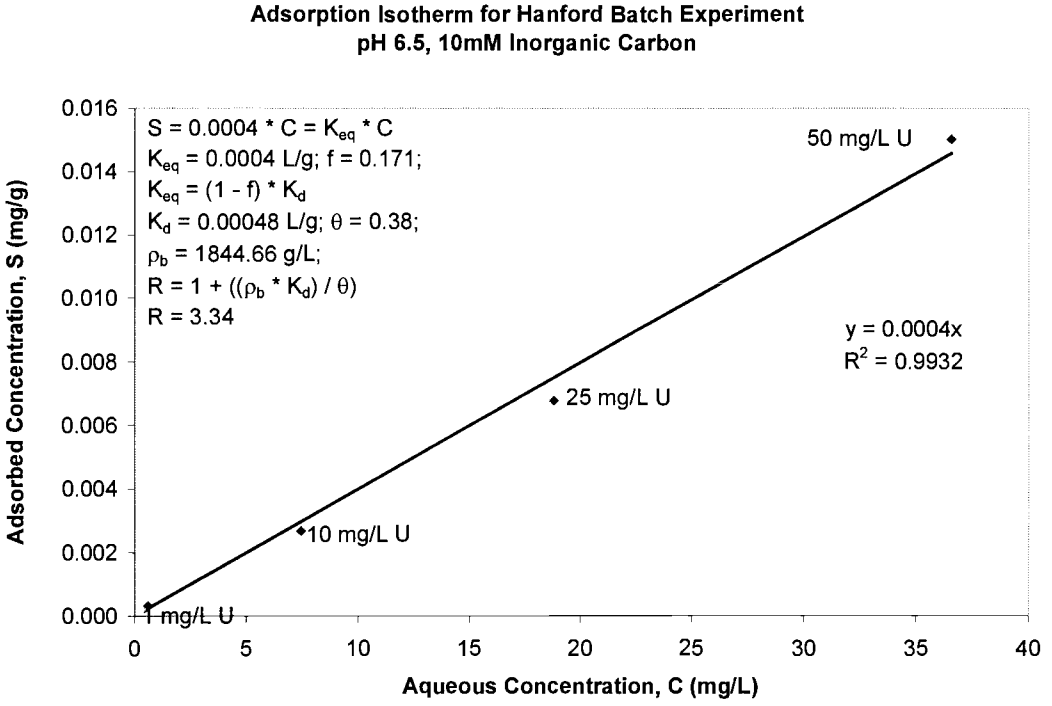

Figure 4: Adsorbed vs. aqueous U concentration for pH 6.5, 10 mM inorganic carbon Hanford batch experiment. Aqueous U is between 1 and 50 ppm, with 0.85 g/ml solid to solution ratio.

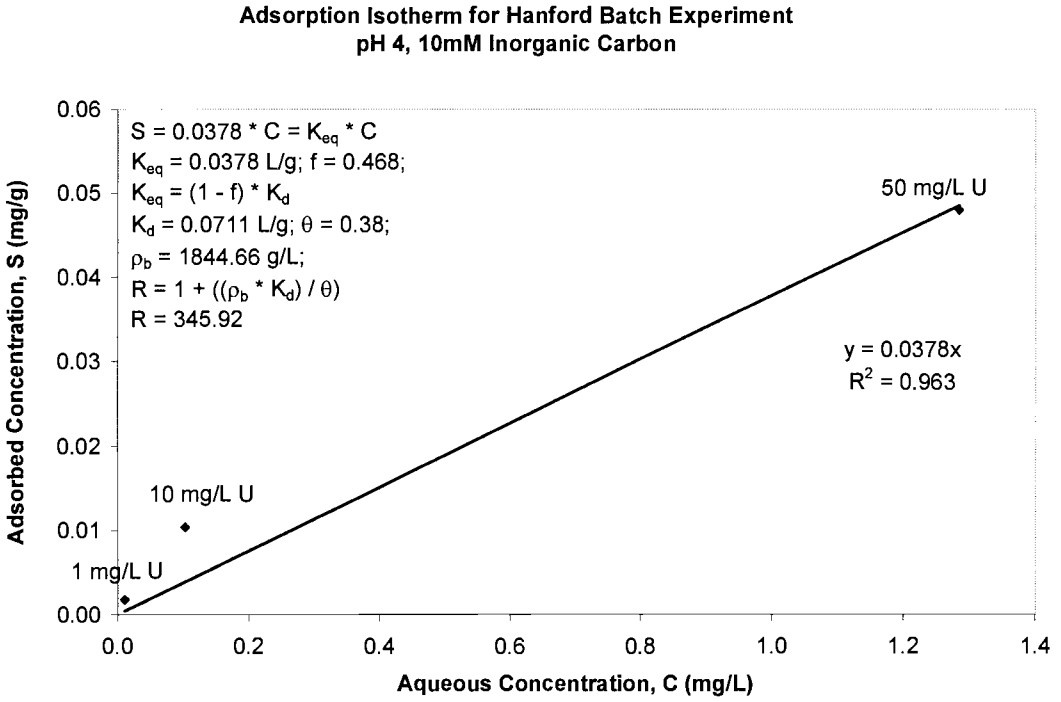

Figure 5: Adsorbed vs. aqueous U concentration for pH 4, 10 mM inorganic carbon Hanford batch experiment. Aqueous U is between 1 and 50 ppm, with 0.9 g/ml solid to solution ratio.

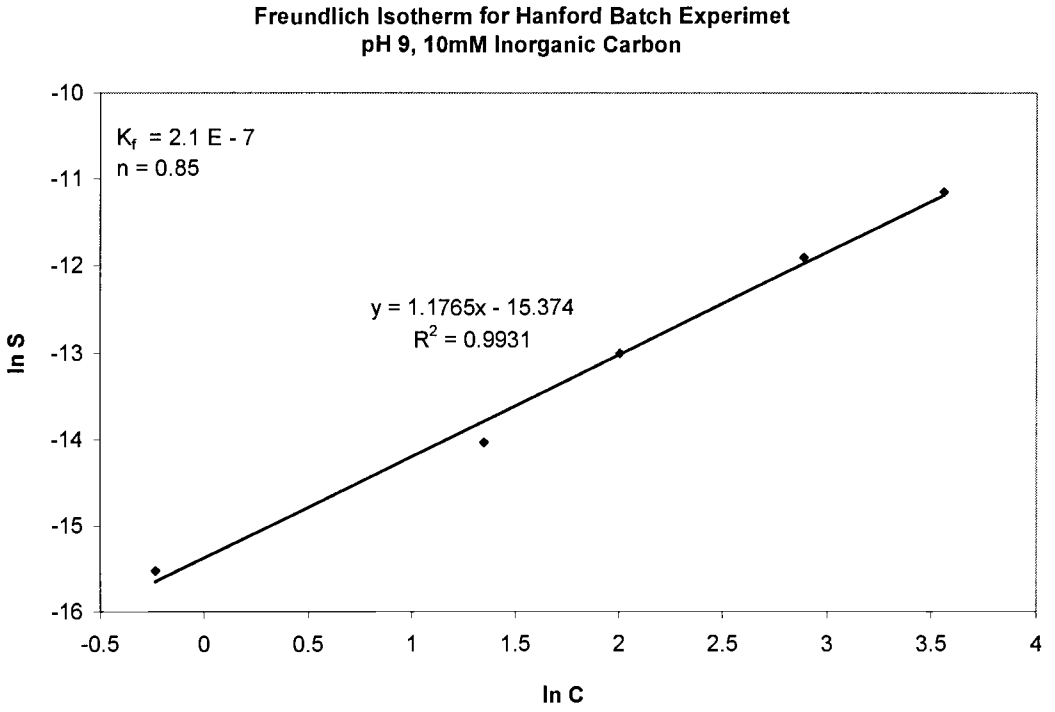

Figure 6: Freundlich isotherm for pH 9, 10 mM inorganic carbon Hanford batch experiment. Uranium concentrations are between 1 and 50 ppm, with 0.8 g/ml solid.

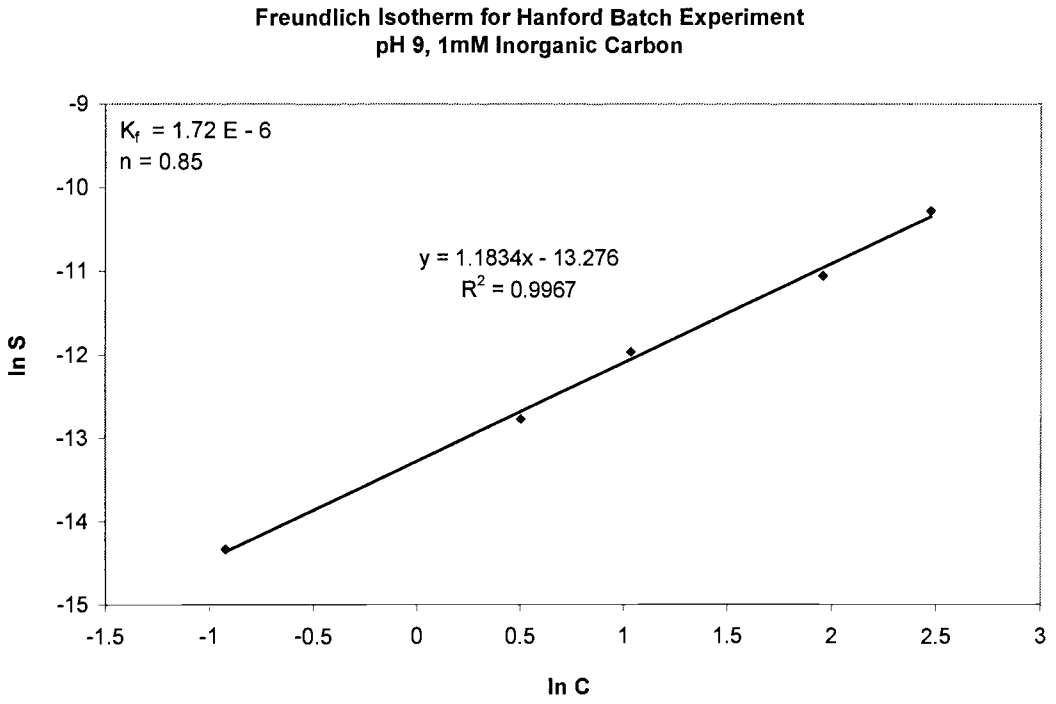

Figure 7: Freundlich isotherm pH 9, 1 mM inorganic carbon for Hanford batch experiment. Uranium concentrations are between 1 and 50 ppm, with 0.8 g/ml solid.

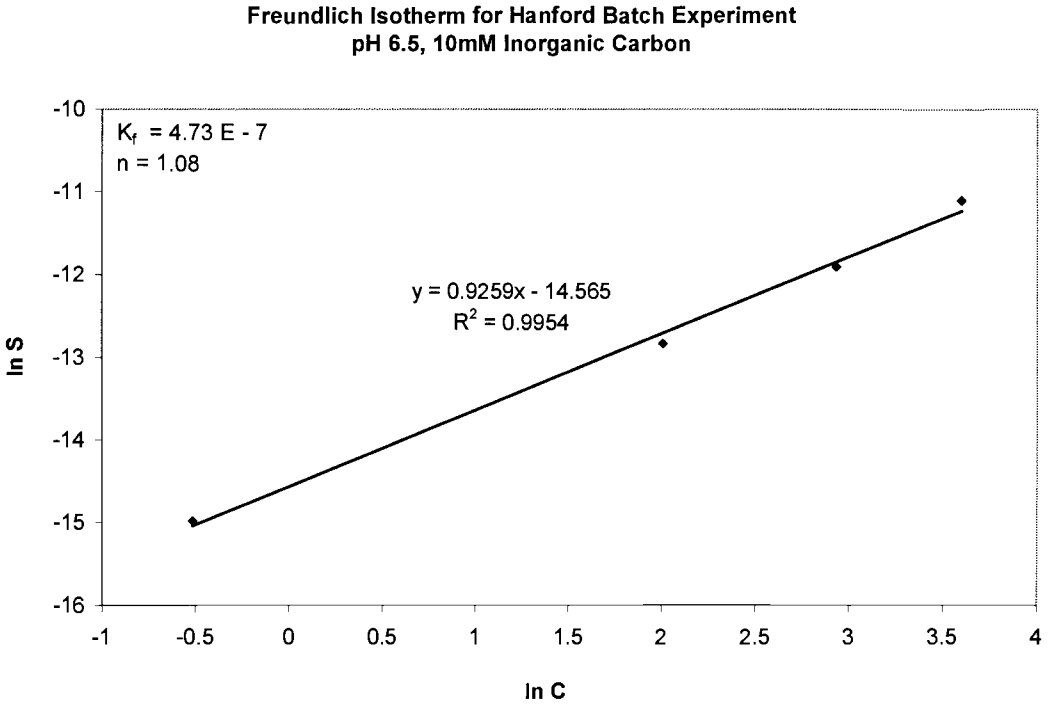

Figure 8: Freundlich isotherm for pH 6.5, 10 mM inorganic carbon Hanford batch experiment. Uranium concentrations are between 1 and 50 ppm, with 0.85 g/ml solid.

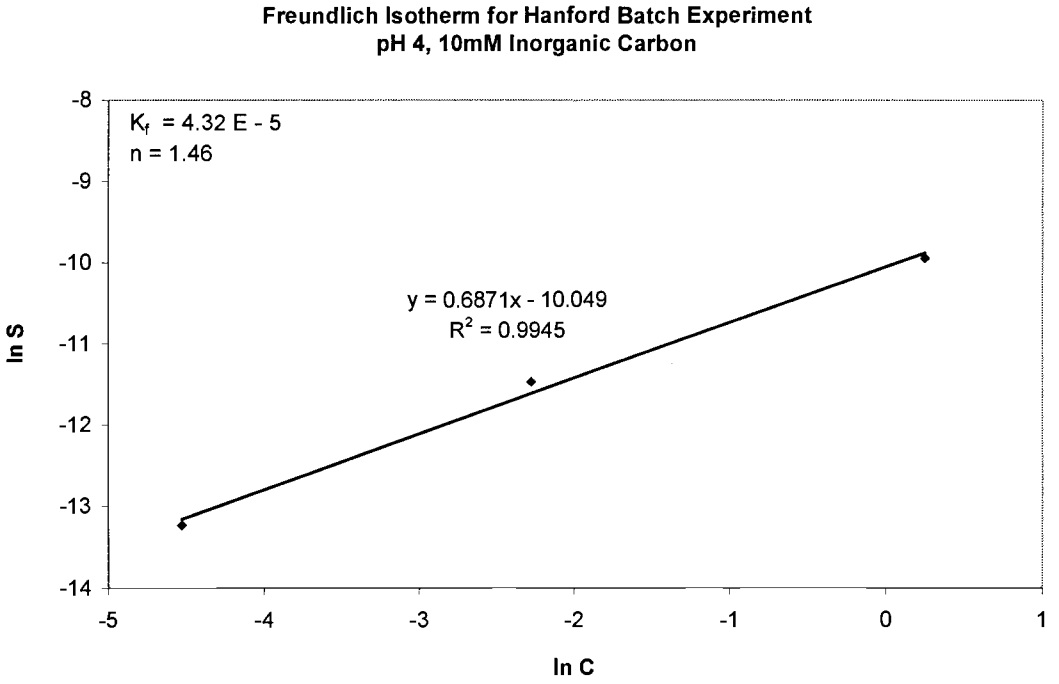

Figure 9: Freundlich isotherm for pH 4, 10 mM inorganic carbon Hanford batch experiment. Uranium concentrations are between 1 and 50 ppm, with 0.9 g/ml solid.

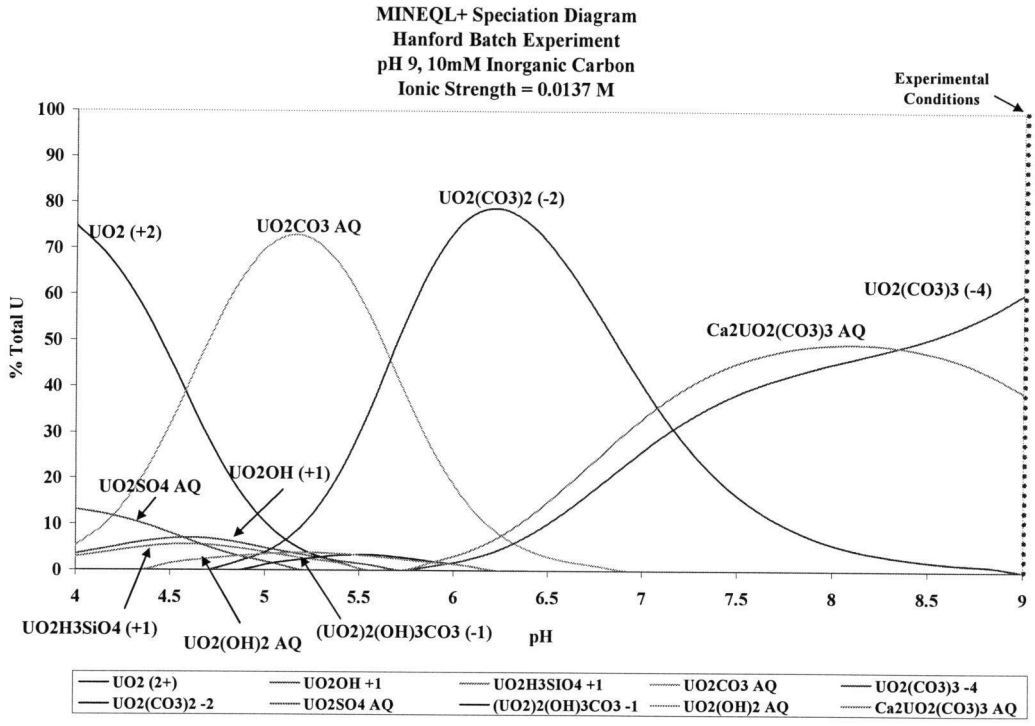

Figure 10: Aqueous speciation diagram for pH 9, 10 mM inorganic carbon batch experiment with 1 mg/L U(VI). Speciation was determined with MINEQL+ as a function of pH using the thermodynamic data from Grenthe et al. (1992). Experiment was conducted at pH 9 with 10 mM inorganic carbon in a closed system. Ionic strength was 0.0137 M (shown with dotted line).

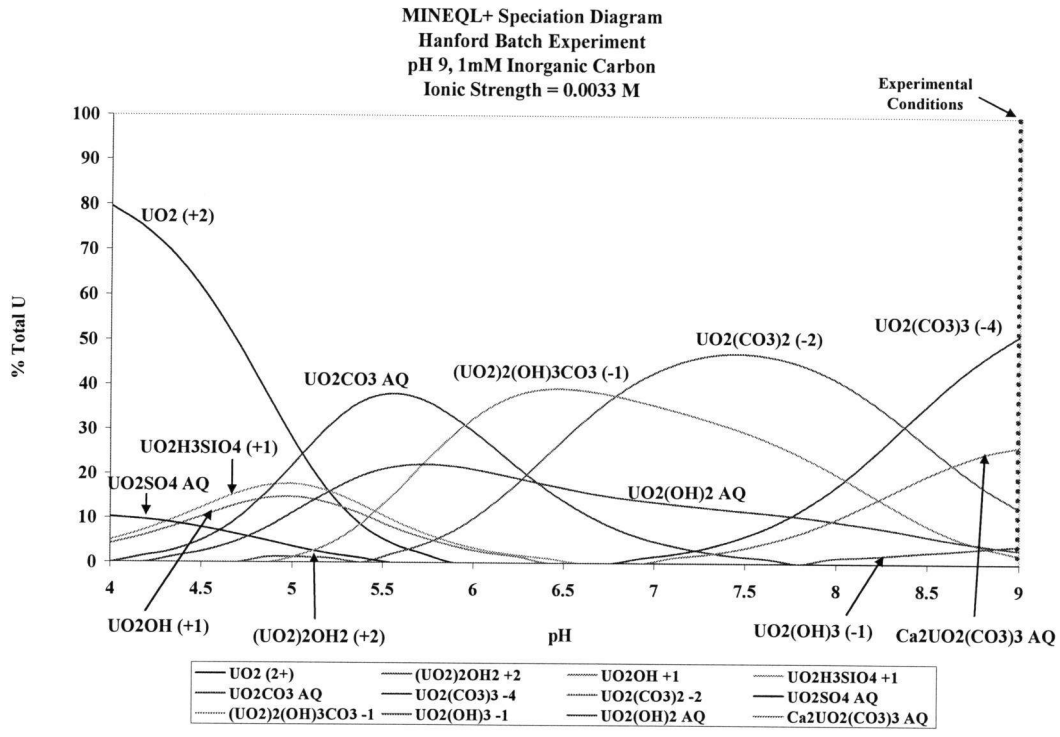

Figure 11: Aqueous speciation diagram for pH 9, 1 mM inorganic carbon batch experiment with 1 mg/L U(VI). Speciation was determined with MINEQL+ as a function of pH using the thermodynamic data from Grenthe et al. (1992). Experiment was conducted at pH 9 with 1 mM inorganic carbon in a closed system. Ionic strength was 0.0033 M (shown with dotted line).

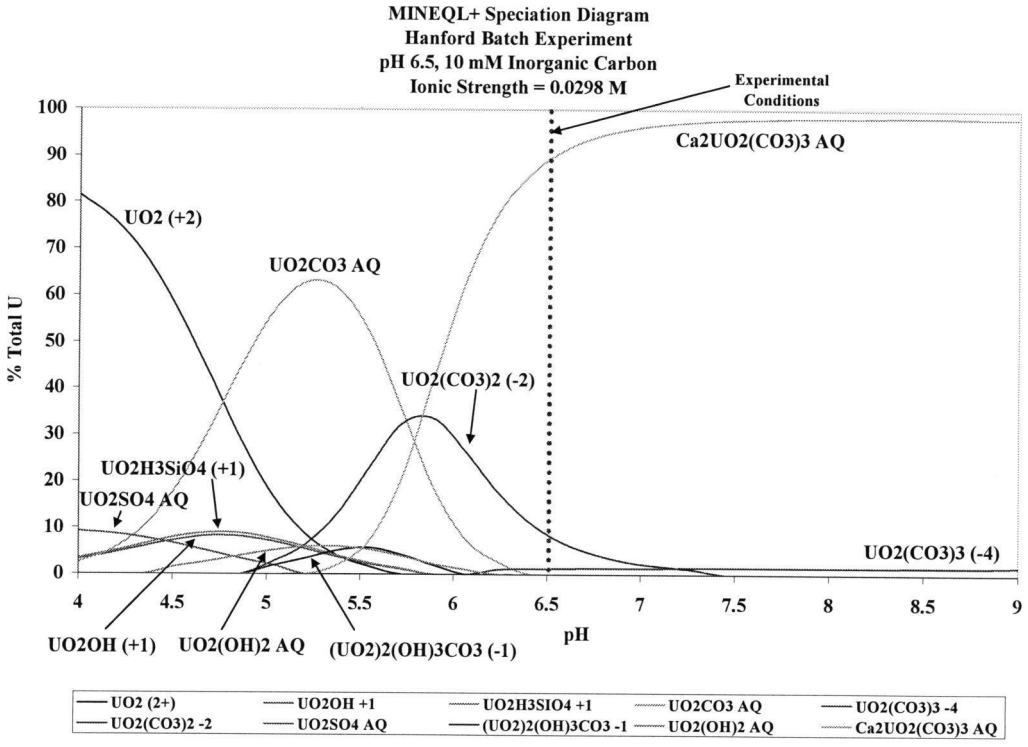

Figure 12: Aqueous speciation diagram for pH 6.5, 10 mM inorganic carbon batch experiment with 1 mg/L U(VI). Speciation was determined with MINEQL+ as a function of pH using the thermodynamic data from Grenthe et al. (1992). Experiment was conducted at pH 6.5 with 10mM inorganic carbon in a closed system. Ionic strength was 0.0298 M (shown with dotted line).

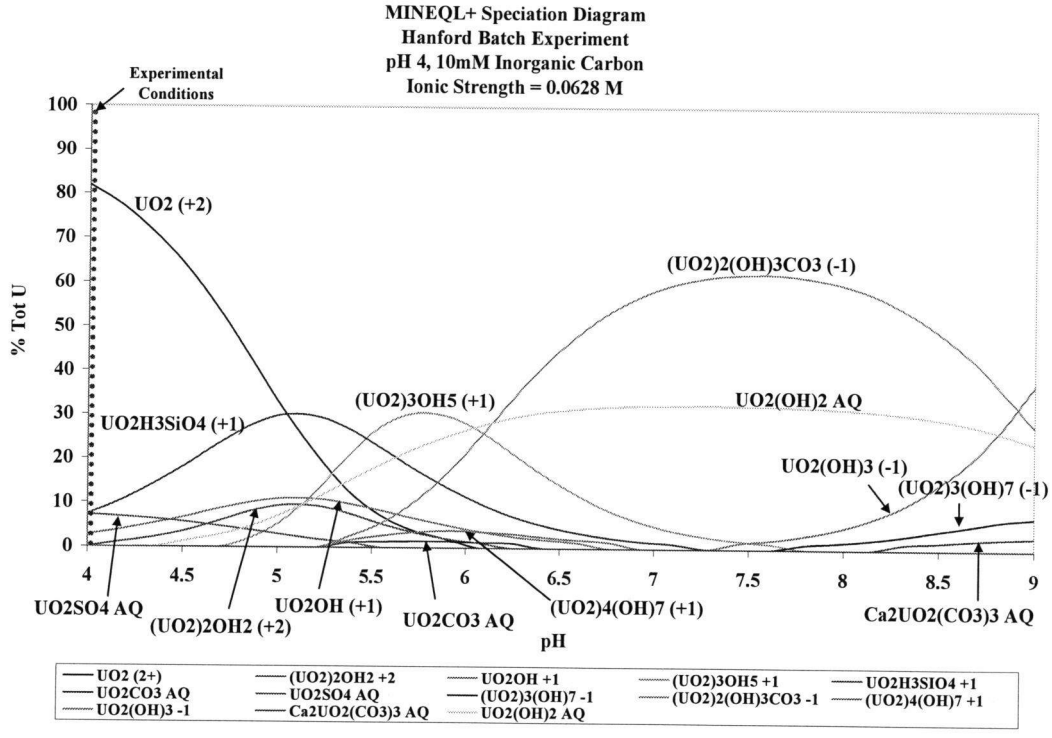

Figure 13: Aqueous speciation diagram for pH 4, 10 mM inorganic carbon batch experiment with 10 mg/L U(VI). Speciation was determined with MINEQL+ as a function of pH using the thermodynamic data from Grenthe et al. (1992). Experiment was conducted at pH 4 with 10 mM inorganic carbon in a closed system. Ionic strength was 0.0628 M (shown with dotted line).

4.2.2. FITEQL Surface Speciation

Total speciation (aqueous plus surface) diagrams were produced for each batch experiment using calculated surface and measured ion concentrations. Surface concentrations of iron minerals were estimated as described by Waite et al. (1994), with a strong site (Fe(s)OH) concentration of 0.0018 moles sites per mole Fe, and weak site (Fe(w)OH) concentration of 0.8732 moles sites per mole Fe (Waite et al. 1994). The following surface site composition (Table 5) was obtained.

Table 5. Surface site compositions calculated from experimental data for FITEQL surface speciation modeling.

Experiment Type	pH	mM Inorg. Carbon	g/L Fe_T	M Fe_T	Fe(s)OH (M)	Fe(w)OH (M)
Batch	4	10	0.8566	9.625E-3	1.7325E-5	8.405E-3
Batch	6.5	10	0.8269	9.291E-3	1.6724E-5	8.113E-3
Batch	9	10	0.7748	8.7056E-3	1.567E-5	7.602E-3
Batch	9	1	0.7364	8.2742E-3	1.4893E-5	7.225E-3
Column	All	All	1.7598	1.977E-2	3.5591E-5	1.727E-2

Using this information, along with the surface reactions shown in Table 6, aqueous species shown in Table 1, ionic strengths calculated from MINEQL+, and ion concentrations (Appendix IV), surface speciation diagrams were developed using FITEQL. The output was transferred to excel and graphed as percent total U vs. pH for each experiment. These are shown in Figures 14 through 17.

Table 6. Ferrihydrite surface reactions from Table 3 of Waite et al. (1994).

SURFACE REACTION EQUATIONS	LOG K VALUE
$FeOH + H^+ <=> FeOH_2^+$	+ 6.51
$FeOH <=> FeO^- + H^+$	- 9.13
$FeOH + H_2CO_3 <=> FeCO_3H + H_2O$	+ 2.90
$FeOH + H_2CO_3 <=> FeCO_3^- + H_2O + H^+$	- 5.09
$(Fe(s)(OH)_2) + UO_2^{2+} <=> (Fe(s)O_2)UO_2 + 2H^+$	- 2.57
$(Fe(w)(OH)_2) + UO_2^{2+} <=> (Fe(w)O_2)UO_2 + 2H^+$	- 6.28
$(Fe(s)(OH)_2) + UO_2^{2+} + H_2CO_3 <=> (Fe(s)O_2)UO_2CO_3^{2-} + 4H^+$	-13.01
$(Fe(w)(OH)_2) + UO_2^{2+} + H_2CO_3 <=> (Fe(w)O_2)UO_2CO_3^{2-} + 4H^+$	-17.10

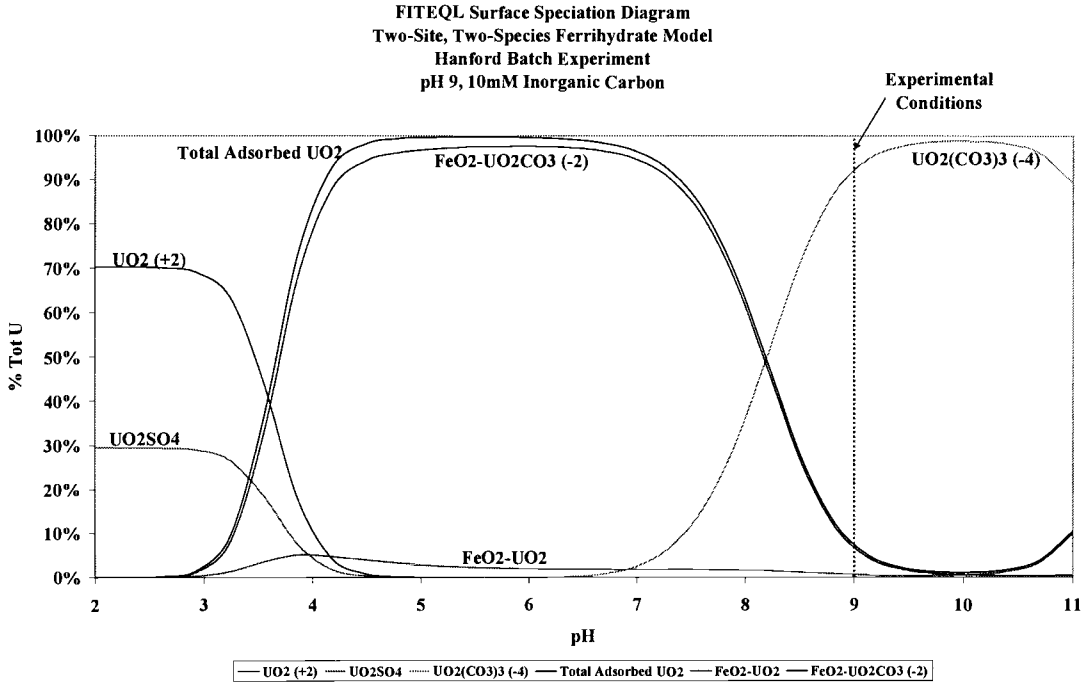

Figure 14: Two-site, two-species iron surface speciation diagram for pH 9, 10 mM inorganic carbon batch experiment with 1 mg/L U(VI). Aqueous speciation from thermodynamic data in Table 1, and surface speciation from reactions shown in Table 6. Experiment was conducted at pH 9 with 10 mM inorganic carbon in a closed system. Ionic strength was 0.0137 M, with strong and weak site concentrations shown in Table 5.

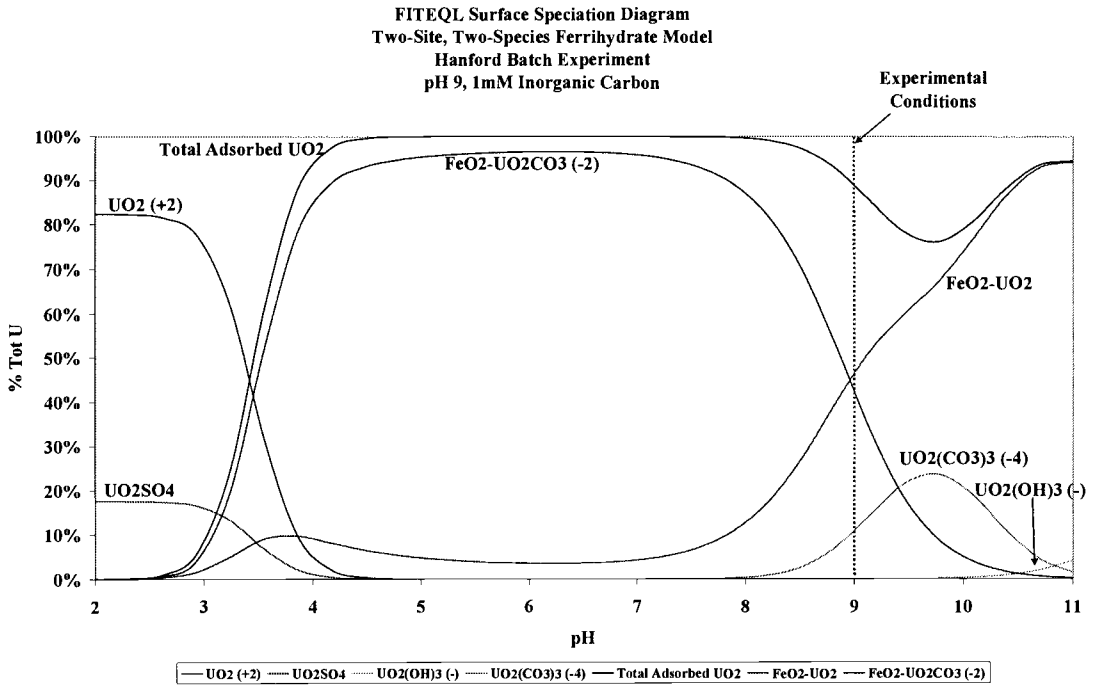

Figure 15: Two-site, two-species iron surface speciation diagram for pH 9, 1 mM inorganic carbon batch experiment with 1 mg/L U(VI). Aqueous speciation from thermodynamic data in Table 1, and surface speciation from reactions shown in Table 6. Experiment was conducted at pH 9 with 1 mM inorganic carbon in a closed system. Ionic strength was 0.0033 M, with strong and weak site concentrations shown in Table 5.

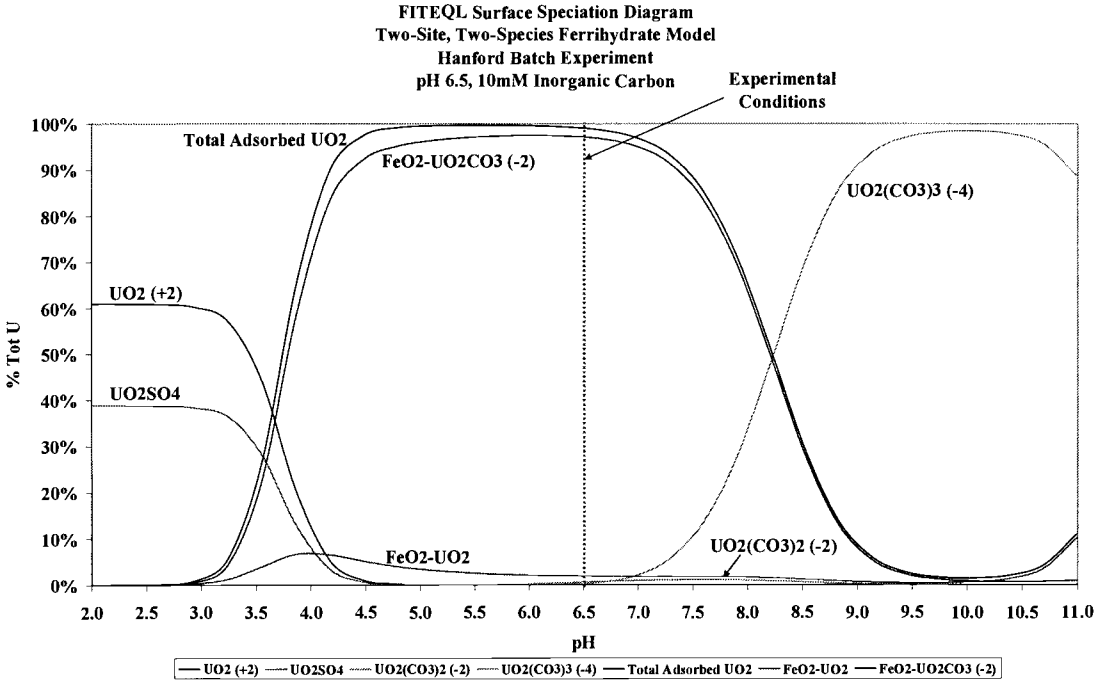

Figure 16: Two-site, two-species iron surface speciation diagram for pH 6.5, 10 mM inorganic carbon batch experiment with 1 mg/L U(VI). Aqueous speciation from thermodynamic data in Table 1, and surface speciation from reactions shown in Table 6. Experiment was conducted at pH 6.5 with 10 mM inorganic carbon in a closed system. Ionic strength was 0.0298 M, with strong and weak site concentrations shown in Table 5.

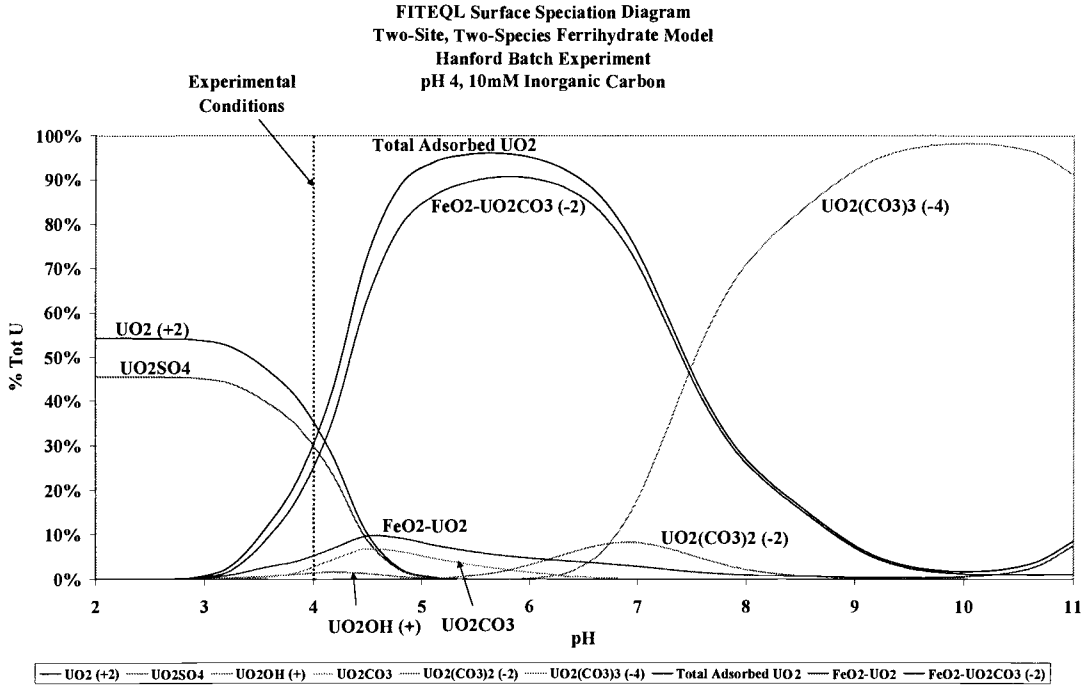

Figure 17: Two-site, two-species iron surface speciation diagram for pH 4, 10 mM inorganic carbon batch experiment with 10 mg/L U(VI). Aqueous speciation from thermodynamic data in Table 1, and surface speciation from reactions shown in Table 6. Experiment was conducted at pH 4 with 10 mM inorganic carbon in a closed system. Ionic strength was 0.0628 M, with strong and weak site concentrations shown in Table 5.

4.3. Column Experimental Results

All transport experiments were conducted using the same column and experimental setup. The experimental setup is shown in Figure 1. Each experiment was run with Hanford groundwater, adjusted to the correct pH and inorganic carbon content. The influent solution containing U and Br were injected for one pore volume, and then the column was flushed with Hanford groundwater until the complete breakthrough curve was obtained. Inorganic carbon and pH were periodically checked throughout the experiments to ensure constant conditions. For the pH 9 and 6.5 experiments, the tracer consisted of 10 ppm U and 300 ppm Br diluted 1:10 with Hanford groundwater. The pH 4 experiment was conducted with 100 ppm U and 3000 ppm Br as tracers, diluted 1:10. The higher concentrations for the pH 4 experiment ensured measurable U concentrations for the resultant breakthrough curve, determined from batch experimental results. Bromide was used in all cases as a conservative tracer to ensure consistency due to its non-reactivity.

4.3.1. Bromide Data and Modeling

Bromide was used as a non-reactive tracer in all transport experiments, with near complete mass recovery within the first four pore volumes. Due to the conservative nature of the resultant Br data, a deterministic equilibrium model was used to fit the data in CXTFIT. Retardation factors (R) were all assumed to be 1, and the flux-averaged concentrations were taken from IC data for the appropriate column experiment. Models were used to fit values for the pore water velocity (v) and the dispersion coefficient (D), with results shown in Table 7.

Table 7. CXTFIT Deterministic Equilibrium CDE Model fits of v and D for Br tracer in Hanford Column Experiments.

Element	pH	mM Inorg. Carbon	Co (mg/cm^3)	v (CXTFIT, cm/min)	D (CXTFIT, cm^2/min)	R (CXTFIT)
Br	9	10	0.0239	0.3119	0.2935	1.0
Br	9	1	0.0239	0.3108	0.2195	1.0
Br	6.5	10	0.0222	0.3347	0.4179	1.0
Br	4	10	0.3054	0.2534	0.352	1.0

4.3.2. Uranium Data and Modeling

The transport of U was analyzed as a function of both pH and inorganic carbon concentrations. Due to the very high retardation values determined from 1 mM inorganic carbon batch experiments; the pH 6.5 and 4 experiments were only run at 10 mM inorganic carbon concentrations. Samples from each column experiment were taken until nearly complete U breakthrough was accomplished. This took anywhere from 4 pore volumes, determined from the pH 9, 10 mM inorganic carbon experiment, to 97 pore volumes, which was the case for the pH 4, 10 mM inorganic carbon experiment.

The resultant U curves were then fit using the deterministic two-site nonequilibrium transport model in CXTFIT. This model assumes that two sites (one at equilibrium and the other being kinetically controlled) are responsible for the adsorption of uranium as total U. In order to fit these data, pore water velocity and dispersion coefficients were used from Br fits, leaving *R*, the partitioning coefficient (β), and the dimensionless mass transfer coefficient (ω) to be fit by the model. The resultant values for these parameters are shown in Table 8.

Table 8. CXTFIT Two-Site Deterministic Non-Equilibrium CDE fits of R, β, and ω for Hanford Column Studies.

Element	pH	mM Inorg. Carbon	Co (ng/cm^3)	v (CXTFIT, cm/min)	D (CXTFIT, cm^2/min)	R (CXTFIT)	β (CXTFIT)	ω (CXTFIT)
U	9	10	903.4	0.3119	0.2935	1.255	0.8379	0.8422
U	9	1	959.76	0.3108	0.2195	4.451	0.3692	1.482
U	6.5	10	1063.7	0.3347	0.4179	14.2	0.2291	2.2
U	4	10	9219.16	0.2534	0.352	33.75	0.4809	2.428

The fits of this model do not take into account multiple species being responsible for the adsorption process, thus leading to inaccurate fits of the breakthrough curves. Resultant U breakthrough curves with corresponding Br tracers are shown in Figures 18 through 21, with all U curves shown together without Br in Figure 22.

4.3.3. MINEQL+ Results for Transport Experiments

Aqueous speciation diagrams were created in MINEQL+ using data gathered from IC and ICP analysis (Appendix V). Major anions, cations, pH, and inorganic carbon concentrations were input into the program, along with the thermodynamic data from Grenthe et al. (1992). The simulations were run as titrations from pH 4 to 9 in a closed system with constant inorganic carbon and pH conditions. The ionic strength was calculated by MINEQL+ for each run based on the information given. Each individual transport experiment resulted in varying aqueous U species present. This did not however show surface speciation, thus leading to the need to use a more appropriate model. The resulting data displays each species as percent total U vs. pH, shown in Figures 23 through 26.

4.3.4. FITEQL Surface Speciation Results for Transport Experiments

Due to the inability of MINEQL+ to have differing mass balance and mass action equations for surface reactions, a more appropriate model was needed to determine surface and aqueous speciation together. FITEQL was run to determine speciation given surface and aqueous reactions, equilibrium constants, aqueous and solid concentrations, and ionic strengths. Aqueous and iron surface speciation data shown in Tables 1 and 6, iron strong and weak surface site concentrations in Table 5, MINEQL ionic strength calculations, and IC and ICP data (Appendix V) were all input into the program. Resultant graphs of percent total U vs. pH for each transport experiment are shown in Figures 27 through 30.

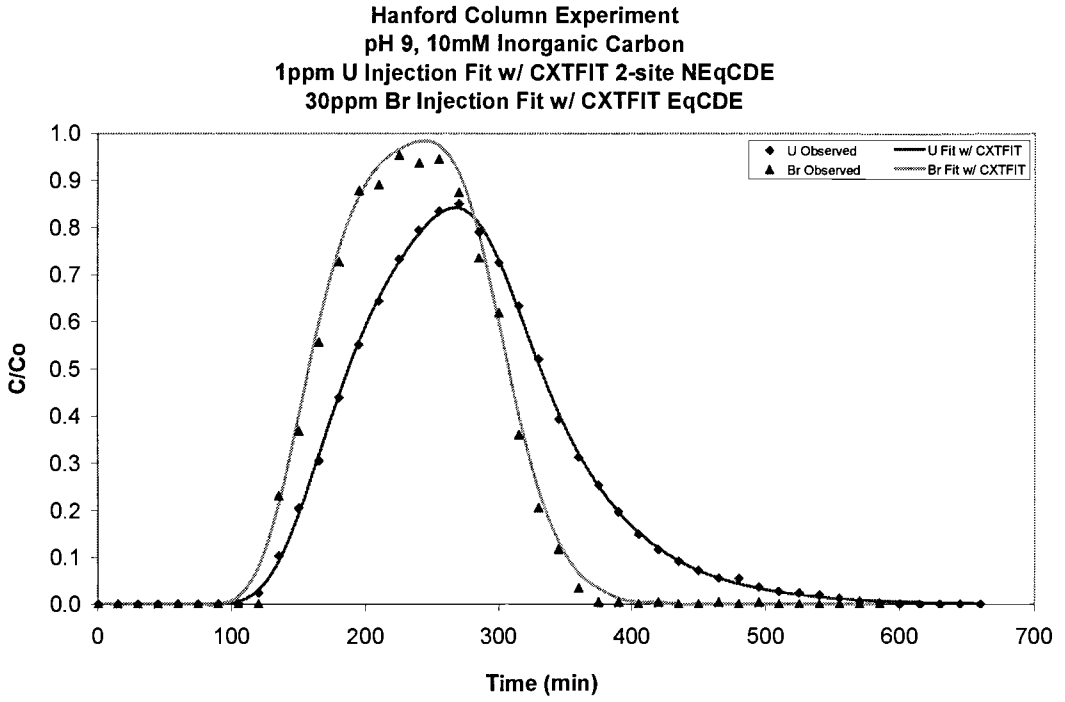

Figure 18: Uranium and Bromide breakthrough curves graphed as C/C_0 vs. time for the pH 9, 10 mM inorganic carbon Hanford column experiment. Measured data are shown as points and model results are shown as lines. Data were fit using CXTFIT.

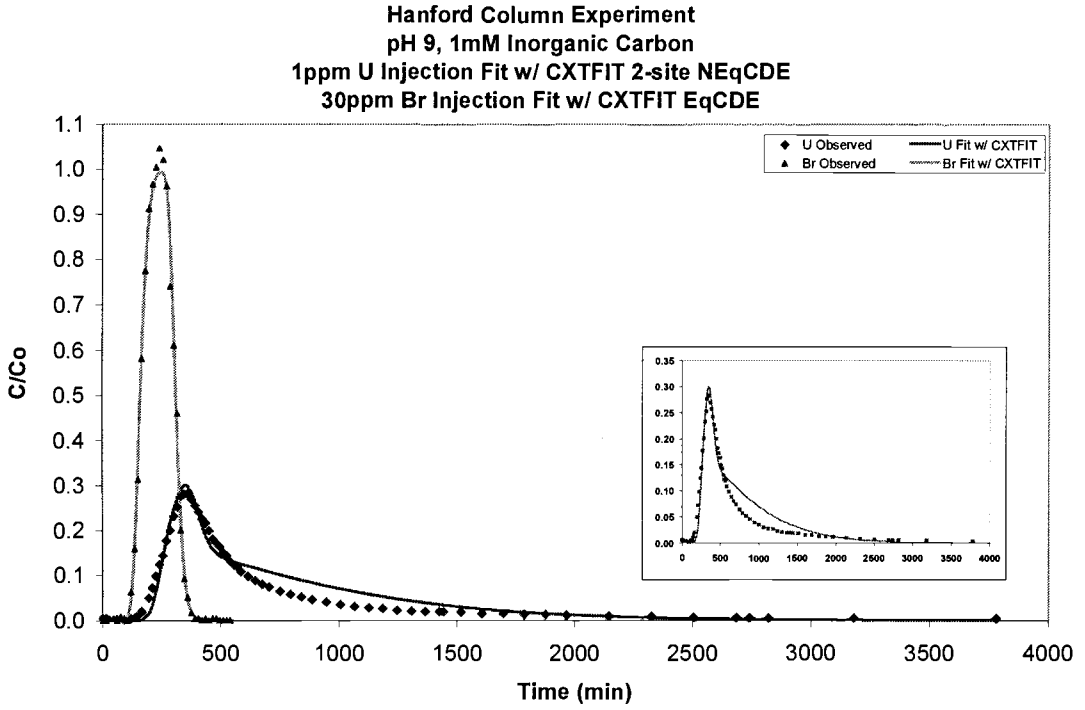

Figure 19: Uranium and Bromide breakthrough curves graphed as C/C_o vs. time for the pH 9, 1 mM inorganic carbon Hanford column experiment. Measured data are shown as points and model results shown as lines. Data are fit using CXTFIT. A plot of the U data with a magnified vertical axis is shown in the inset.

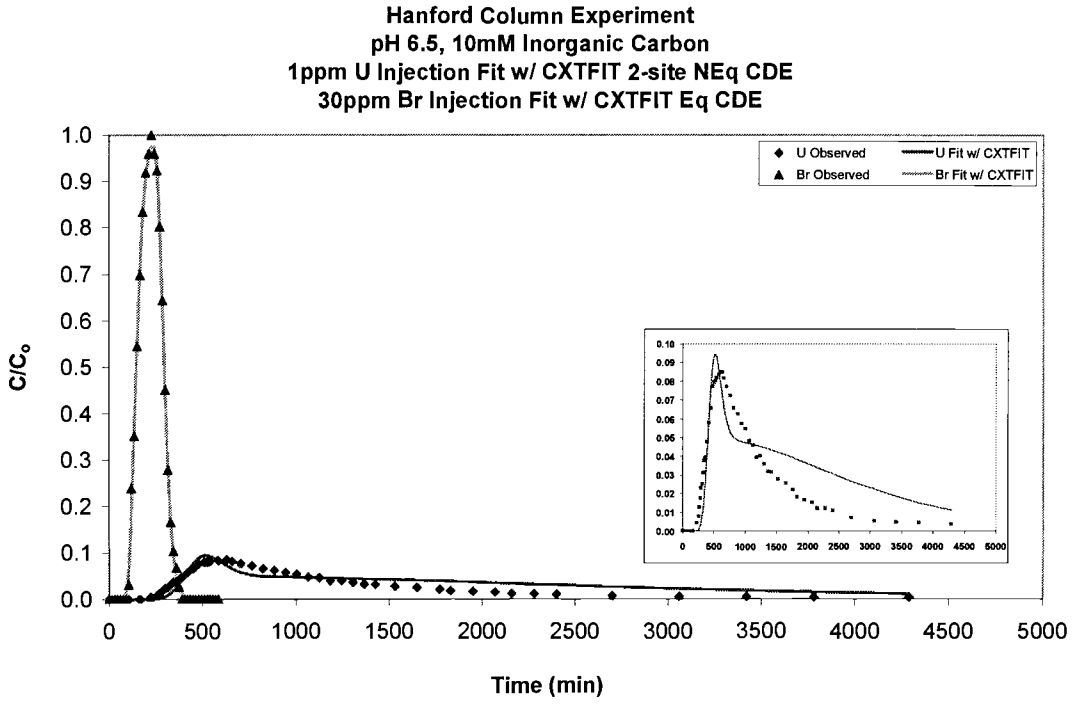

Figure 20: Uranium and Bromide breakthrough curves graphed as C/Co vs. time for the pH 6.5, 10 mM inorganic carbon Hanford column experiment. Measured data are shown as points and model results shown as lines. Data are fit using CXTFIT. A plot of the U data with a magnified vertical axis is shown in the inset.

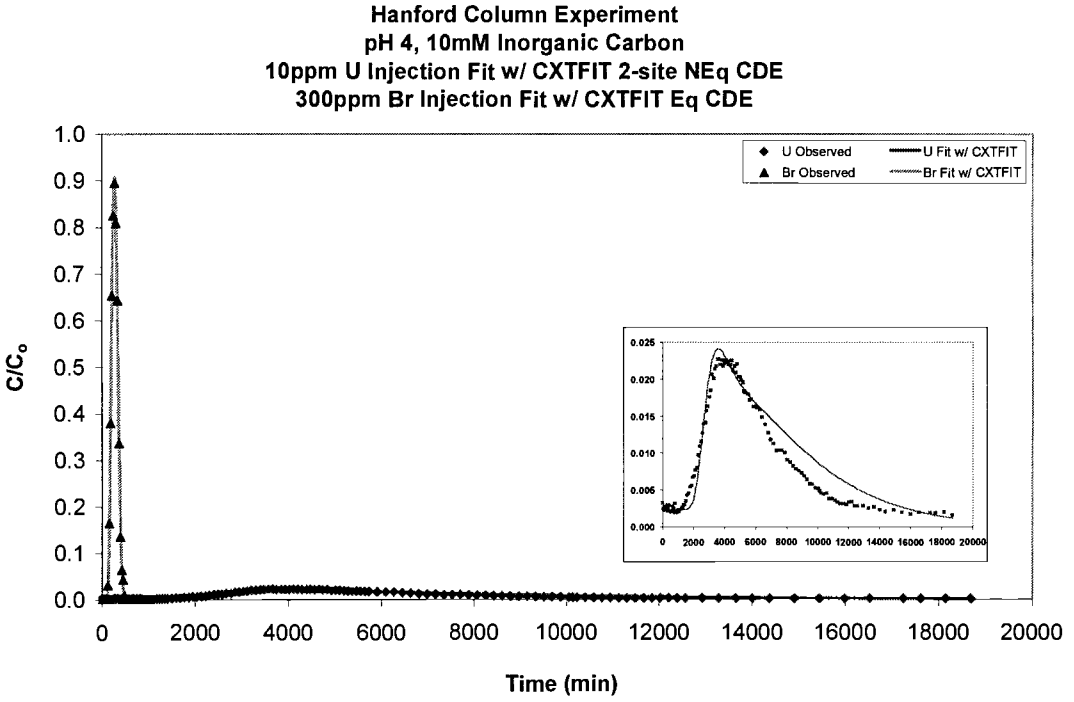

Figure 21: Uranium and Bromide breakthrough curves graphed as C/C_o vs. time for the pH 4, 10 mM inorganic carbon Hanford column experiment. Measured data are shown as points and model results shown as lines. Data are fit using CXTFIT. A plot of the U data with a magnified vertical axis is shown in the inset.

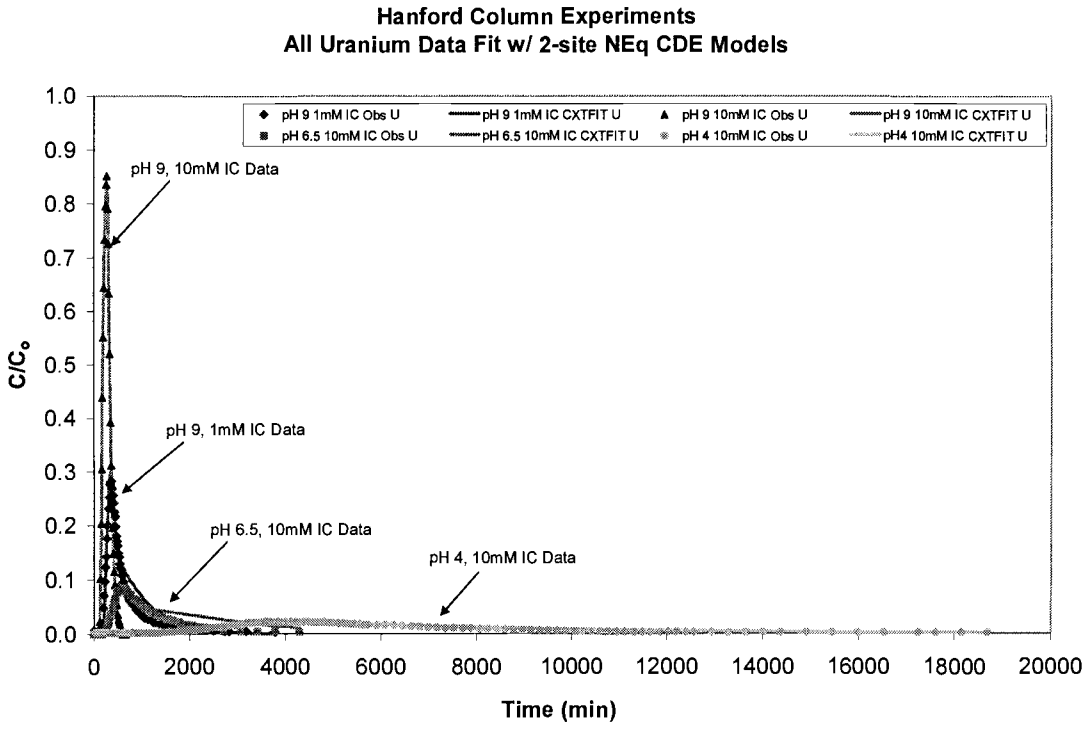

Figure 22: Uranium breakthrough curves graphed as C/C_o vs. time for all Hanford column experiment. Measured data are shown as points and model results shown as lines. Data were fit using the deterministic two-site nonequilibrium CDE model in CXTFIT.

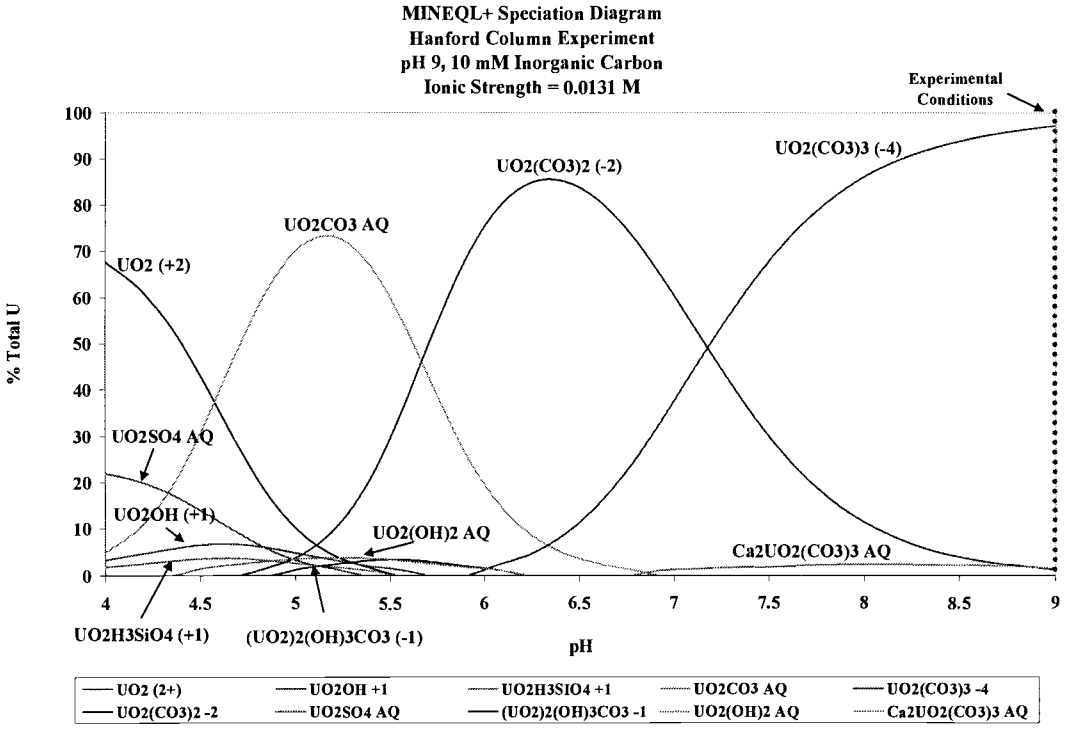

Figure 23: Aqueous speciation diagram for pH 9, 10 mM inorganic carbon column experiment with 1 mg/L U(VI). Speciation was determined with MINEQL+ as a function of pH using the thermodynamic data from Grenthe et al. (1992). Experiment was conducted at pH 9 with 10 mM inorganic carbon in a closed system. Ionic strength was 0.0131 M (shown with dotted line).

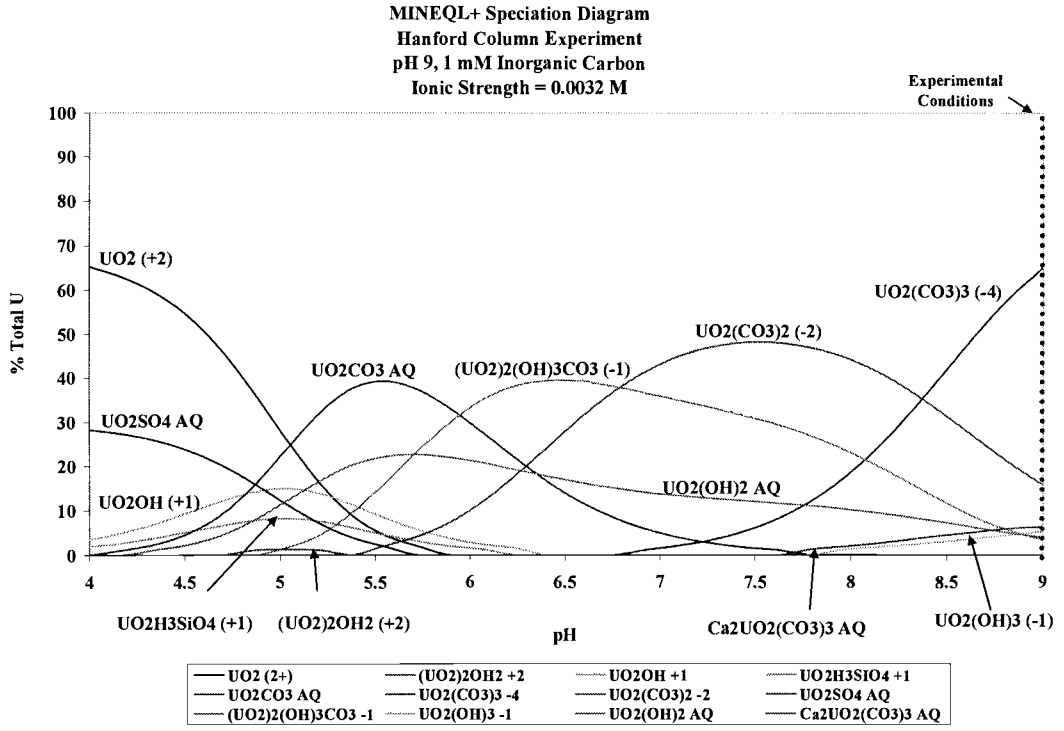

Figure 24: Aqueous speciation diagram for pH 9, 1 mM inorganic carbon column experiment with 1 mg/L U(VI). Speciation was determined with MINEQL+ as a function of pH using the thermodynamic data from Grenthe et al. (1992). Experiment was conducted at pH 9 with 1 mM inorganic carbon in a closed system. Ionic strength was 0.0032 M (shown with dotted line).

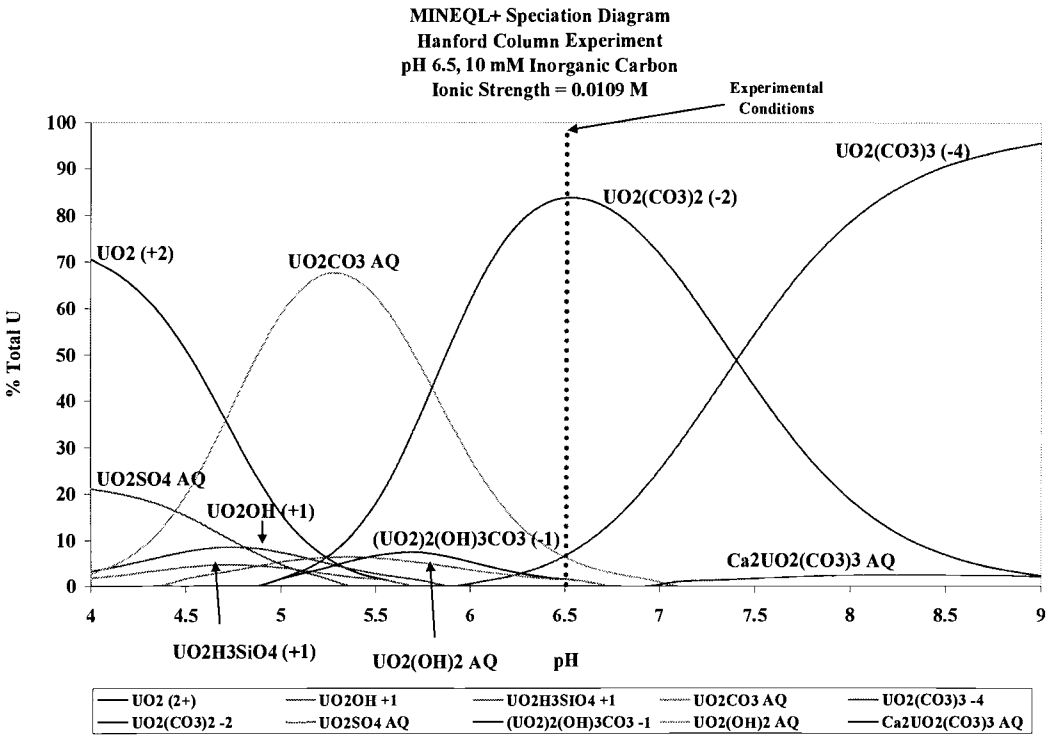

Figure 25: Aqueous speciation diagram for pH 6.5, 10 mM inorganic carbon column experiment with 1 mg/L U(VI). Speciation was determined with MINEQL+ as a function of pH using the thermodynamic data from Grenthe et al. (1992). Experiment was conducted at pH 6.5 with 10 mM inorganic carbon in a closed system. Ionic strength was 0.0109 M (shown with dotted line).

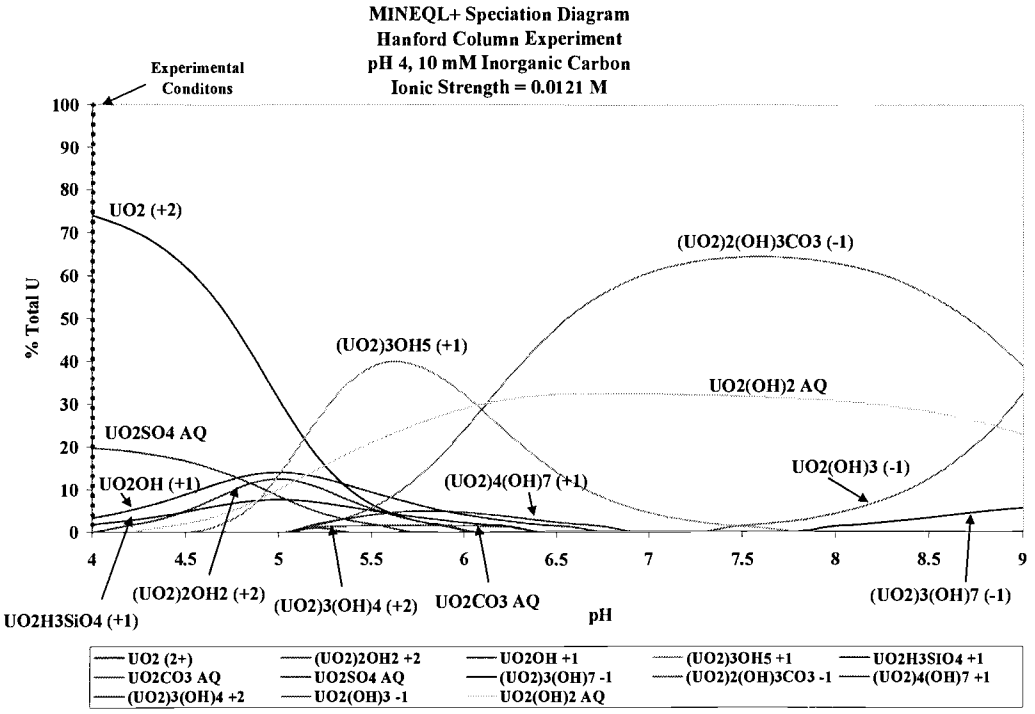

Figure 26: Aqueous speciation diagram for pH 4, 10 mM inorganic carbon column experiment with 10 mg/L U(VI). Speciation was determined with MINEQL+ as a function of pH using the thermodynamic data from Grenthe et al. (1992). Experiment was conducted at pH 4 with 10 mM inorganic carbon in a closed system. Ionic strength was 0.0121 M (shown with dotted line).

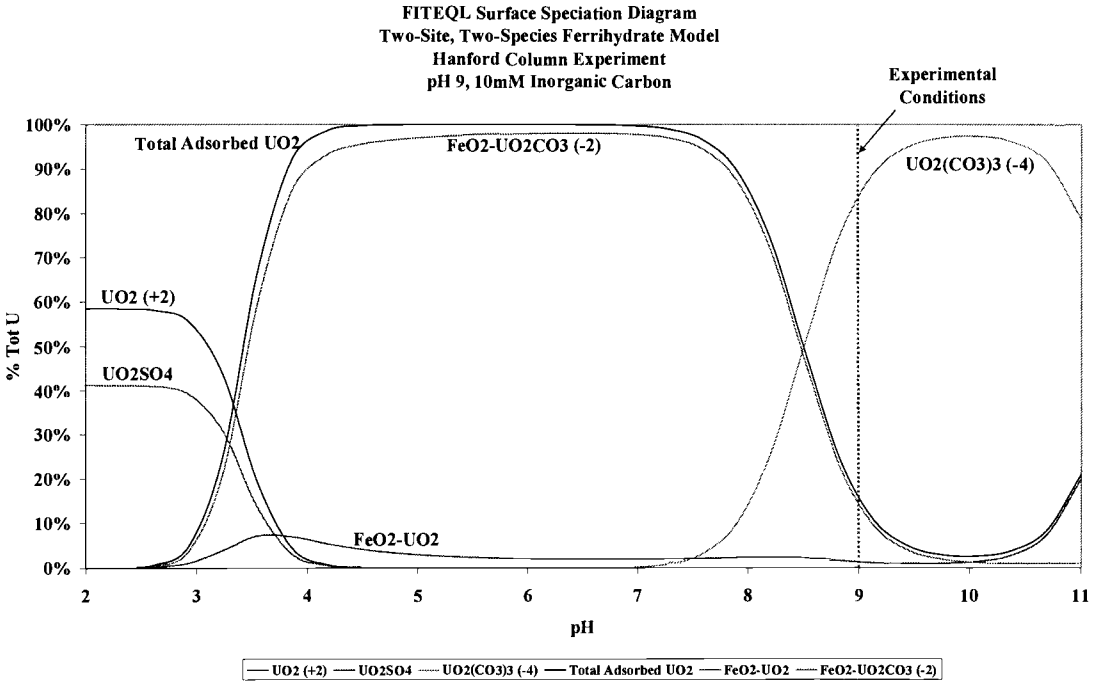

Figure 27: Two-site, two-species iron surface speciation diagram for pH 9, 10 mM inorganic carbon column experiment with 1 mg/L U(VI). Aqueous speciation from thermodynamic data in Table 1, and surface speciation from reactions shown in Table 6. Experiment was conducted at pH 9 with 10 mM inorganic carbon in a closed system. Ionic strength was 0.0131 M, with strong and weak site concentrations shown in Table 5.

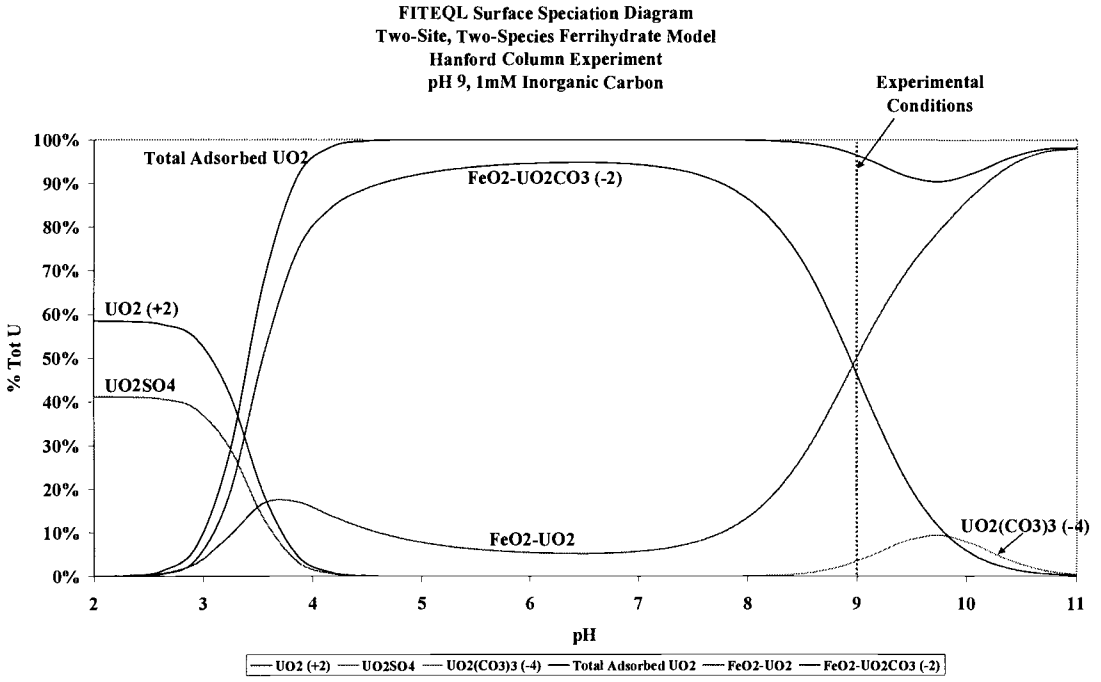

Figure 28: Two-site, two-species iron surface speciation diagram for pH 9, 1 mM inorganic carbon column experiment with 1 mg/L U(VI). Aqueous speciation from thermodynamic data in Table 1, and surface speciation from reactions shown in Table 6. Experiment was conducted at pH 9 with 1 mM inorganic carbon in a closed system. Ionic strength was 0.0032 M, with strong and weak site concentrations shown in Table 5.

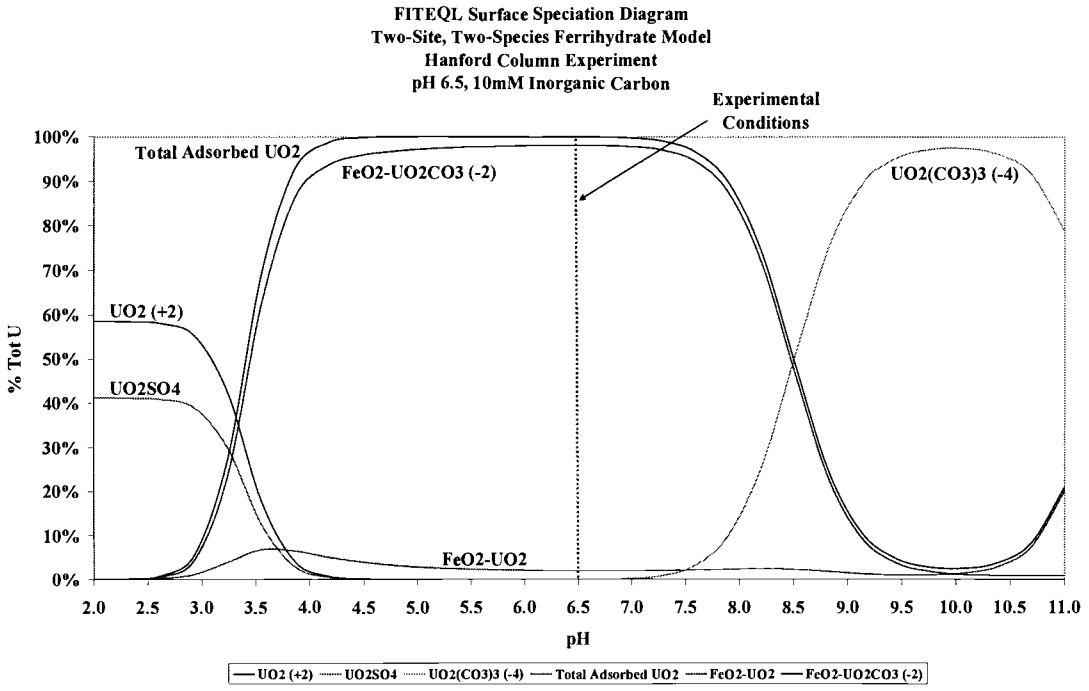

Figure 29: Two-site, two-species iron surface speciation diagram for pH 6.5, 10 mM inorganic carbon column experiment with 1 mg/L U(VI). Aqueous speciation from thermodynamic data in Table 1, and surface speciation from reactions shown in Table 6. Experiment was conducted at pH 6.5 with 10 mM inorganic carbon in a closed system. Ionic strength was 0.0109 M, with strong and weak site concentrations shown in Table 5.

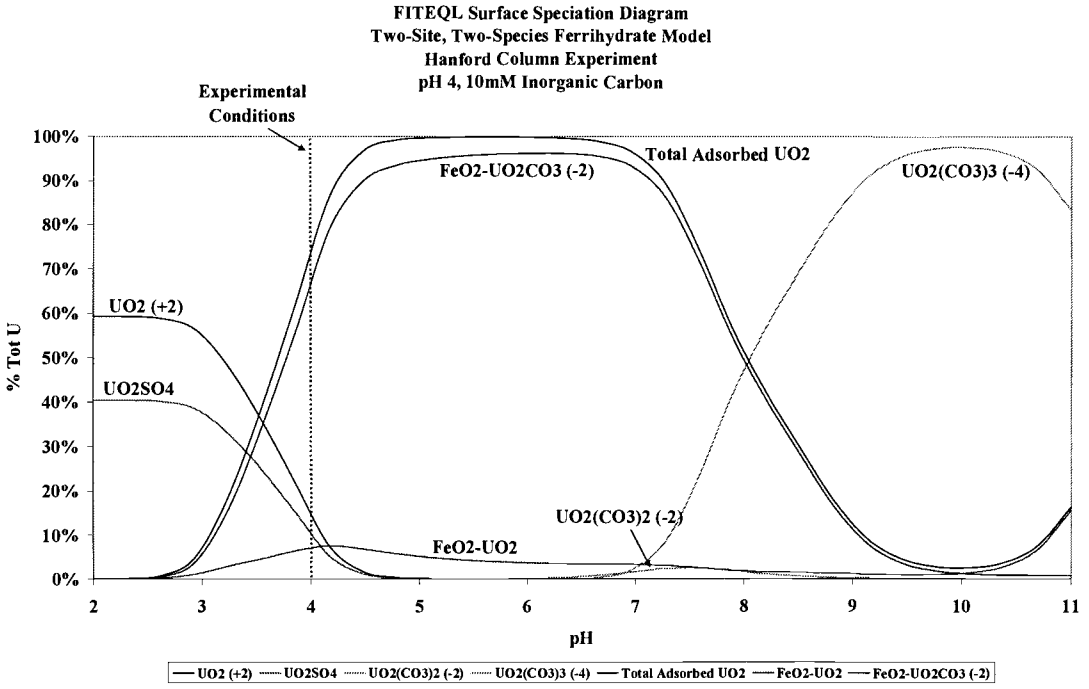

Figure 30: Two-site, two-species iron surface speciation diagram for pH 4, 10 mM inorganic carbon column experiment with 10 mg/L U(VI). Aqueous speciation from thermodynamic data in Table 1, and surface speciation from reactions shown in Table 6. Experiment was conducted at pH 4 with 10 mM inorganic carbon in a closed system. Ionic strength was 0.0121 M, with strong and weak site concentrations shown in Table 5.

5. DISCUSSION

5.1. Batch Kinetic Experiments

Concentrations of dissolved U in all batch experiments reached equilibrium within the 960 minutes, with near complete adsorption occurring within the first four hours. The largest amount of adsorption (98.97%) occurred in the pH 4, 10 mM inorganic carbon batch, which had the highest ionic strength and up to two orders of magnitude higher aqueous calcium concentrations than did other experiments. The pH 9, 1 mM inorganic carbon batch had 60.26% adsorbed U, the pH 6.5, 10 mM inorganic carbon batch had 40.42% adsorbed U, and the pH 9, 10 mM inorganic carbon batch had 20.97% adsorbed U. This indicated that as either the sediment pH or the inorganic carbon concentration decreases, more U will adsorb to surface sites.

The increase in adsorption with the reduction in pH is not consistent with the FITEQL simulations. There are several possible reasons for this, including (1) the influence of aqueous and adsorbed species that were not accounted for in the model, and (2) the removal of solid carbonate and silicate minerals from the sediment with the addition of the nitric acid that was used for pH adjustment. Ions, such as calcium and silica, were not included in FITEQL simulations due to the lack of thorough knowledge in how U complexes with these in both aqueous and solid phases. Including the aqueous phase reactions for these ions without the knowledge of how U reacts with them in the solid phase resulted in even greater errors then when they were completely excluded from the model. With the removal of these solid phases from the sediment, more surface sites may be uncovered leading to higher strong and weak site concentrations than would normally be present for the sediment. This hypothesis can be rationalized by the presence of aqueous calcium and silica concentrations (Appendix IV), as well as the gas production observed in the bottles upon the addition of nitric acid during the equilibration process.

As inorganic carbon concentrations were decreased in the pH 9 batch experiments, the amount of adsorption increased. The likely explanation for this is that as more CO_3^{2-}

was present in the alkaline pH range, the formation of aqueous U-carbonate complexes decreased the amount of adsorption due to competition between surface and aqueous complexes (Waite et al. 1994). The ionic strength was also much lower at the lower inorganic carbon concentration. Observations by Waite et al. (1994) and Barnett et al. (2000) suggested a slight dependence on ionic strength in the alkaline pH range, with more adsorption occurring with a reduction in ionic strength.

5.1.1. Batch Isotherms

Adsorption isotherms were plotted in two ways, as a linear adsorption isotherm (Figures 2 through 5) and as a nonlinear Freundlich isotherm (Figures 6 through 9). Both resulted in good fits, with R^2 values above 0.9. The Freundlich isotherms provided slightly better fits to the data, indicating the possibility of a nonlinear relationship between the amounts of U adsorbed and dissolved U concentrations. This trend has been seen in other research, including Barnett et al. (2000) and Waite et al. (1994). The Freundlich isotherm may suggest that multiple sites are responsible for the adsorption of U species, or that multiple types of adsorbing species are present. However, the least-squared residuals for both the linear and Freundlich isotherms were approximately of the same order of magnitude, suggesting that for these data either model would be acceptable.

5.1.2. MINEQL+ Aqueous Speciation Diagrams

Aqueous speciation diagrams were predicted by MINEQL+, as well as calculations for ionic strengths for each experiment. In analyzing the resulting percent total U vs. pH diagrams (see Figures 10 through 13), high concentrations of aqueous U-silica (Figure 13) and U-calcium-carbonato (Figures 10 through 12) species were present at each of the experimental conditions. This indicated that both silica and calcium play an important role in the complexation of U. Without a thorough knowledge in how silica and calcium complex with U, these species could not be adequately described in a system with both solid and aqueous phases present. Thus, both calcium and silica species were omitted in the further modeling of aqueous and surface speciation by FITEQL.

5.1.3. FITEQL Surface Speciation Diagrams

FITEQL surface speciation diagrams were modeled using the same aqueous equilibrium data as used in the MINEQL+ model, with the addition of surface reactions described in Table 6 (Waite et al. 1994). The calcium and silica species were removed, since their adsorption chemistry is currently unknown. The model was run as a closed system with constant inorganic carbon concentration over the pH range from 2 to 11. The resulting graphs of percent total U vs. pH are shown in Figures 14 through 17.

These graphs show both aqueous and adsorbed species at each experimental pair of pH and inorganic carbon. The amount of adsorption predicted by the model did not completely represent that seen in experiments, reflecting the presence of potential uncertainties in modeling the chemical system, the actual state of the system chemistry, or both. These uncertainties could include many aspects of both the system and modeling. The amounts of strong and weak surface sites were calculated using the information detailed in Waite et al. (1994), which may not necessarily be accurate for the sediment used in these experiments. Since the sediment in batch experiments was pre-equilibrated to various pH and inorganic carbon concentrations, amounts of nitric acid were added to change the natural conditions of the sediment to those for each experiment. This resulted in dissolved silicate and carbonate minerals from the surface of the sediment, potentially exposing additional adsorption sites. Also, the effects of silica and calcium complexes with U were not introduced into the surface complexation model due to uncertainties in their surface complexation. An understanding of this may improve modeling fits to the experimental data.

5.2. Transport Experiments

Uranium transport experiments showed increased adsorption with both decreases in pH and inorganic carbon concentrations. As can be seen in Figure 22, the highest amount of adsorption was again in the pH 4, 10 mM inorganic carbon experiment. The pH 6.5, 10 mM inorganic carbon experiment was next, followed by the pH 9, 1 mM and then 10 mM inorganic carbon experiments. The increase in adsorption with decrease in

pH may be due to the increase in available surface sites by removal of solid carbonate and silicate minerals from the sediment, as was hypothesized for the batch experiments. As the equilibrium sediment and aqueous phase pH and inorganic carbon concentration was lowered, these solids may have been dissolved from the surface exposing new surface sites that may have led to increased adsorption of U species.

5.2.1. CXTFIT Modeling

CXTFIT was used in to fit both U and Br breakthrough curves using the models given by Equations 3 and 4 for U, and Equation 1 for Br. The U data was fit using a two-site non-equilibrium model, which assumed that two different types of surface sites were responsible for adsorption, one site being at equilibrium and the other being kinetically controlled. It was assumed that the pore-water velocity and dispersion coefficient were the same for both Br and U, so the fits of these variables for the U data were set to the values obtained in the Br data set. The results are shown in Figures 18 through 21; the U curves on the same plot in Figure 22. As can be seen from these figures, the Br data was well described by the equilibrium model (Equation 1). The pH 9, 10 mM inorganic carbon U data was well modeled by the two-equation model (Equations 3 and 4). The fits of all other U transport data was not nearly as accurate. This may be due to the model assumption that only a single species is involved in the reactive transport. Due to the inability to account for multiple aqueous and surface species, the reactive transport model fits were inaccurate. A different reactive transport model might improve the ability to simulate the observed U data.

5.2.2. FITEQL Surface Speciation Diagrams

The adsorption seen in transport experiments was well reproduced with FITEQL surface speciation diagrams (for these simulations, MINEQL+ was first used with the ion concentration data and thermodynamic database shown in Appendix V and Table 1 to calculate the ionic strength). The percentage of adsorption tend to be higher than was seen from the resultant data, with the exception being the fit for the pH 4, 10 mM

inorganic carbon experimental data which is less than is expected from results. FITEQL models can be found in Figures 27 through 30. Absolute errors in model fits are at most 25% from experimental data. This may be due to the removal of aqueous calcium and silica from the modeled system, or the increase in available strong and weak surface sites as carbonate and silicate minerals were removed from the sediment. There may also be other surface species contributing to the adsorption or dissolution of U that have not been taken into consideration due to lack of knowledge.

The aqueous species responsible for the decrease in adsorption in the alkaline pH range is shown in both pH 9 speciation diagrams as $UO_2(CO_3)_3^{4-}$. This species has more of an effect at higher inorganic carbon concentrations, with the decrease in adsorption between pH 7 and 10 for 10^{-2} mM total inorganic carbon and only between pH 8 and 9.75 for 10^{-3} mM total inorganic carbon. The amount of adsorption increases near pH 10 due to the hypothesized inability of carbonate to compete for U with the highly negative surface sites in this range (Barnett et al. 2002).

In the acidic pH range, aqueous UO_2^{2+} and UO_2SO_4 compete with surface sites for U complexation. These species become less dominant in the range between pH 2.5 and 5, where surface sites begin to appear. For the pH 4, 10 mM inorganic carbon transport experiment, the concentrations of strong and weak sites used is most likely inaccurate due to the removal of solids from the sediment surface during the equilibration to this acidic pH. This leads to the potential for an increase in strong and weak surface binding sites, where the resulting amount of U adsorption increases proportionally to the number of available surface sites.

6. CONCLUSION

Uranium transport in subsurface environments is a complicated process, with many aqueous and surface complexes being formed. In this study, the effects of pH and inorganic carbon on the adsorption of U to Hanford sediment was studied through the use of both batch and transport experiments to better understand how these parameters play a role in both U speciation and U adsorption to the solid phase.

Batch experiments were performed to analyze the effects of varying U concentrations on adsorption. The results provided information about the amount of adsorption that might be seen in transport studies, as well as showed the effects of pH and inorganic carbon on the adsorption of U to Hanford sediment. As either pH or inorganic carbon was decreased, the amount of U adsorption increased. Experimental results were fit with both linear and nonlinear adsorption isotherms; the nonlinear Freundlich isotherm was a slightly better fit. This was consistent with equilibrium modeling of the geochemical system, which suggested that both multiple species and surface sites were responsible for adsorption.

Transport experiments were conducted to see if kinetic adsorption effects could be observed. The results generally agreed with the batch studies, with the amount of adsorption increasing with a decrease in equilibrium pH or inorganic carbon. The reactive transport for experimental U data was determined using the two-site nonequilibrium model in CXTFIT. The results showed near one hundred percent recovery of U in all cases. The transport model showed a good fit for the pH 9, 10 mM inorganic carbon breakthrough curve, but was not adequate for the other three transport experiments. The assumption for these cases is that it is important to consider the multiple U species explicitly, as well as potentially more than two distinct surface sites being responsible for the adsorption process.

The effects of pH and inorganic carbon on adsorption in this study can be rationalized by the hypotheses stated in the introduction section of this thesis. These three hypotheses were: (1) changes in pH from alkaline to the acidic range would affect the adsorption of U; (2) changes in inorganic carbon from high concentration (10mM) to

low concentration (1mM) would affect the adsorption of U; and (3) the presence of multiple mineral phases may affect the adsorption of U. In analyzing the results of this research, it was determined that in reducing the pH during the sediment equilibration process, carbonate and silicate minerals were possibly removed from the surface of the sediment. This is supported by IC and ICP analysis of the batch and column effluents (Appendix IV and V respectively). With the removal of mineral phases, there may have been an increase in available adsorption sites for U (exposed by mineral dissolution). With an increase in surface binding sites, the amount of U adsorption would increase proportionally. Similarly, as the amount of total inorganic carbon was reduced, carbon from the surface may have been removed during the sediment equilibration process. This was clearly seen in batch equilibration, where the solution off-gassed during the equilibration process. This would also potentially increase the number of surface binding sites available for the adsorption of U. There are also several aqueous phase processes occurring that might affect U adsorption. For example, as the aqueous concentration of inorganic carbon is increased and more U-carbonate complexes are formed in the alkaline pH range, the amount of adsorption will decrease due to competition for U speciation between aqueous and surface sites. Also, as the inorganic carbon concentration is decreased, the measured ionic strength is an order of magnitude lower. Both Waite et al. (1994) and Barnett et al. (2000) have shown a slight dependence of adsorption on ionic strength in the alkaline pH range, with adsorption increasing as ionic strength is lowered.

Aqueous and surface complexation models, MINEQL+ and FITEQL, were used both for batch and transport studies to get an understanding of which species were present in these environments, and to determine if the two-site, two-species model from Waite et al. (1994) would sufficiently describe experimental results in this study. Aqueous speciation diagrams from MINEQL+ calculated the ionic strengths of the systems, as well as determined the aqueous speciation of U for each batch and transport experiment. It also gave a preliminary estimate of which aqueous U species may be responsible for U adsorption. With the implementation of the two-site, two-species model from Waite et al. (1994), UO_2^{2+} and $UO_2CO_3^0$ were assumed to be the two aqueous complexes responsible for U adsorption to the strong and weak iron surface sites on the sediment. These surface

species reactions (Table 6) were added to the surface complexation model created in FITEQL to show how well these species described what was happening in comparison to experimental results.

Batch MINEQL+ diagrams showed the large effects calcium had on the aqueous speciation of U in the pH 6.5 and 9 results. The U-calcium-carbonato complex was the dominant or near dominant species for these cases, leading to the need for a better understanding of how this complex and solid calcium play a role in the U adsorption process. Dissolved silicate may have also played a role in the aqueous speciation and adsorption of U. Silica species showed up in the neutral to acidic pH range in all MINEQL+ batch diagrams, at times forming up to 10% of the aqueous species (e.g., the pH 4, 10 mM inorganic carbon system). Whether solid U-silica species are playing a role in the adsorption of U in this system is unknown due to a lack of thorough knowledge in this area.

Aqueous speciation diagrams for transport studies showed much lower concentrations of aqueous U-calcium-carbonato and U-silica species. These species played little to no role in the aqueous MINEQL+ speciation diagrams. Since dissolving or desorbing species are continually removed from a flowing system, lower concentrations of U-calcium-carbonato and U-silica species were measured in the effluent.

The two species responsible for surface reactions were hypothesized to be the UO_2^{2+} and $UO_2CO_3^0$ aqueous species, as described by Waite et al. (1994). Reasonable fits to experimental data were obtained using the surface complexation model of Waite et al. (1994). The simulation results somewhat followed the same trend as the experimental data (the exception again being the pH 4 experiment), although deviations between the predicted vs. experimental results did occur. This may be due to (1) inadequate information on the exact number of strong and weak surface binding sites available in all experimental systems, since these were changed as the sediment was equilibrated prior to each experiment, and (2) calcium and silica aqueous and solid phase reactions that were not thoroughly understood and therefore not included in the model. Overall this model was a good start to understanding U surface complexation, and with improved

information about the number of surface sites available a likely improvement may occur with model simulations.

The primary improvement that could be made for modeling the results of this study would be information on the relationship between the numbers of surface sites and pH as the solid-phase minerals are dissolved or adsorbed species desorb. This would improve surface modeling parameters and give a better idea of how well the two speciation models used in this study actually fit the experimental results. It is evident that there are multiple sites and species responsible for the adsorption of U to Hanford sediment under the varying experimental conditions, and the two-site, two-species FITEQL model with data from Waite et al. (1994) seems to be a good starting point in understanding surface reactions. A different transport model is needed as well to better fit U breakthrough curves from transport experiments, with the incorporation of not only multiple surface sites, but also multiple adsorbing chemical species.

The transport of U(VI) in subsurface environments is very complex. With the research that is being conducted on the aqueous and surface complexes that form, there is an increase in the understanding of what may be happening in subsurface environments. The problem is that with doing research in the lab, one can only predict what would potentially occur in the field. Natural systems have an even more complex array of variables, including multiple minerals, aqueous chemistries, sediment properties (including varying dispersions and pore-water velocities), and organic materials that may contribute to how U reacts in the subsurface. Therefore, lab results may never be perfectly accurate in predicting what will happen in the field. It can only be hoped that ultimately enough information will be gathered to develop a simplified predictive model of what can be expected to occur in various natural environments.

BIBLIOGRAPHY

Bargar, J., et al. (1999). "Spectroscopic Confirmation of Uranium(VI)-Carbonato Adsorption Complexes on Hematite." Environmental Science and Technology **33**(14): 2481-2484.

Bargar, J., et al. (2000). "Characterization of U(VI)-carbonato ternary complexes on hematite: EXAFS and electrophoretic mobility measurements." Geochimica et Cosmochimica Acta **64**(16): 2737-2749.

Barnett, M., et al. (2002). "U(VI) Adsorption to Heterogeneous Subsurface Media: Applications of a Surface Complexation Model." Environmental Science and Technology **36**(5): 937-942.

Barnett, M., et al. (2000). "Adsorption and Transport of Uranium(VI) in Subsurface Media." Soil Sci. Soc. Am **64**: 908-917.

Bostick, B., et al. (2002). "Uranyl Surface Complexes Formed on Subsurface Media from DOE Facilities." Soil Soc. Am **66**: 99-108.

Gabriel, U., et al. (1998). "Reactive transport of uranyl in a goethite column: an experimental and modeling study." Chemical Geology **151**: 107-128.

Gamerdinger, A., et al. (2001). "Two-region flow and decreased sorption of uranium (VI) during transport in Hanford groundwater and unsaturated sands." Water Resources Research **37**(12): 3155-3162.

Grenthe, I., et al. (1992). Chemical Thermodynamics of Uranium. New York, NY, Elsevier Science Publishing Company Inc.

Herbelin, A. and J. Westall (1999). FITEQL: A Computer Program for Determination of Chemical Equilibrium Constants from Experimental Data. Corvallis, OR, Westall, John C.

Hsi, C. and D. Langmuir (1985). "Adsorption of uranyl onto ferric oxyhydroxides: Application of the surface complexation site-binding model." Geochimica et Cosmochimica Acta **49**: 1931-1941.

Kelly, S., et al. (2003). "Uranyl Incorporation in Natural Calcite." Environmental Science and Technology **37**(7): 1284-1287.

Moyes, L., et al. (2000). "Uranium Uptake from Aqueous Solution by Interaction with Goethite, Lepidocrocite, Muscovite, and Mackinawite: An X-ray Absorption Spectroscopy Study." Environmental Science and Technology **34**(6): 1062-1068.

BIBLIOGRAPHY (Continued)

Schecher, W. D.-P. and D. C.-P. McAvoy (1998). MINEQL+: A Chemical Equilibrium Modeling System. Hallowell, Maine, Environmental Research Software.

Toride, N., et al. (1999). The CXTFIT Code for Estimating Transport Parameters from Laboratory or Field Tracer Experiments. Riverside, CA, US Salinity Laboratory, USDA, ARS.

Waite, T., et al. (1994). "Uranium(VI) adsorption to ferrihydrite: Application of a surface complexation model." Geochimica et Cosmochimica Acta **58**(24): 5465-5478.

Wazne, M., et al. (2003). "Carbonate Effects on Hexavalent Uranium Adsorption by Iron Oxyhydroxide." Environmental Science and Technology **37**(16): 3619-3624.

Zheng, Z., et al. (2003). "Influence of Calcium Carbonate on U(VI) Sorption to Soils." Environmental Science and Technology **37**(24): 5603-5608.

APPENDICIES

I. Uncontaminated synthetic Hanford groundwater recipe with 1 and 10 mM inorganic carbon concentrations.

Synthetic Hanford Groundwater w/o Br at 1mM CO_3			
Chemical	**mg/L**	**MW (mg/mmol)**	**mmol/L**
NaCl	15.0	58.4425	0.2567
KCl	8.2	74.5510	0.1100
Na_2SO_4	71.0	142.0431	0.4998
$NaHCO_3$	84.0	84.0069	1.0000
	MW (mg/mmol)	**mmol/L**	mg/L (ppm)
Na^+	22.9898	2.2564	51.8732
K^+	39.0983	0.1100	4.3005
H^+	1.0079	1.0000	1.0079
Cl^-	35.4527	0.3667	12.9989
SO_4^-	96.0636	0.4998	48.0172
CO_3^{2-}	60.0092	1.0000	60.0092

Synthetic Hanford Groundwater w/o Br at 10mM CO_3			
Chemical	**mg/L**	**MW (mg/mmol)**	**mmol/L**
NaCl	15.0	58.4425	0.2567
KCl	8.2	74.5510	0.1100
Na_2SO_4	71.0	142.0431	0.4998
$NaHCO_3$	841.0	84.0069	10.0111
	MW (mg/mmol)	**mmol/L**	mg/L (ppm)
Na^+	22.9898	11.2674	259.0353
K^+	39.0983	0.1100	4.3005
H^+	1.0079	10.0111	10.0906
Cl^-	35.4527	0.3667	12.9989
SO_4^-	96.0636	0.4998	48.0172
CO_3^{2-}	60.0092	10.0111	600.7570

II. Synthetic Hanford groundwater recipe for both 1 and 10 mM inorganic carbon concentrations including U and Br tracer.

Synthetic Hanford Groundwater w/ Br at 1mM CO3			
Chemical	**mg/L**	**MW (mg/mmol)**	**mmol/L**
NaCl	15.0	58.4425	0.2567
KCl	8.2	74.5510	0.1100
Na_2SO_4	71.0	142.0431	0.4998
$NaHCO_3$	84.0	84.0069	1.0000
KBr	44.7	119.0023	0.3756
UO_2^{2+}	1.0	270.0277	0.0037
	MW (mg/mmol)	**mmol/L**	mg/L (ppm)
Na^+	22.9898	2.2564	51.8732
K^+	39.0983	0.4856	18.9867
H^+	1.0079	1.0000	1.0079
UO_2^{2+}	270.0277	0.0037	1.0000
Cl^-	35.4527	0.3667	12.9989
SO_4^-	96.0636	0.4998	48.0172
CO_3^{2-}	60.0092	1.0000	60.0092
Br^-	79.9040	0.3756	30.0138

Synthetic Hanford Groundwater w/ Br at 10mM CO_3			
Chemical	**mg/L**	**MW (mg/mmol)**	**mmol/L**
NaCl	15.0	58.4425	0.2567
KCl	8.2	74.5510	0.1100
Na_2SO_4	71.0	142.0431	0.4998
$NaHCO_3$	841.0	84.0069	10.0111
KBr	44.7	119.0023	0.3756
UO_2^{2+}	1.0	270.0277	0.0037
	MW (mg/mmol)	**mmol/L**	mg/L (ppm)
Na^+	22.9898	11.2674	259.0353
K^+	39.0983	0.4856	18.9867
H^+	1.0079	10.0111	10.0906
UO_2^{2+}	270.0277	0.0037	1.0000
Cl^-	35.4527	0.3667	12.9989
SO_4^-	96.0636	0.4998	48.0172
CO_3^{2-}	60.0092	10.0111	600.7570
Br^-	79.9040	0.3756	30.0138

III. Elements of U measurement interference for kinetic phosphorescence analyzer, with potential effects and maximum tolerance levels.

Element	Potential Effect	Maximum Tolerance, ppm
Aluminum	Quenching	50
Barium	Quenching	1000
Cadmium	Quenching	500
Calcium	Quenching	500
Chloride	Quenching	18
Chromium	Quenching	0.2
Cobalt	Quenching	1
Copper	Quenching	0.5
Fluoride	Etching of Sample Cell	
Iron	Quenching	25
Magnesium	Quenching	250
Manganese	Quenching	3
Methanol	Quenching	0
Nickel	Quenching	10
Potassium	Quenching	5000
Sodium	Quenching	5000
Strontium	Quenching	1000
Zinc	Quenching	500
Zirconium	Precipitate	
TOC	Quenching &/or Fluorescence	
pH	Improper complexing w/ "URAPLEX'	Adjust to pH=1 w/ HNO_3

IV. Measured ion concentrations for batch experiments using IC and ICP, with corresponding charge balance and ionic strength calculations.

4,10 Batch			Charge Balance	Ionic Strength
	Conc.(M)	z	(z*M)	(z^2*M)
Ca	1.97E-02	2	3.94E-02	7.88E-02
K	5.65E-04	1	5.65E-04	5.65E-04
Na	4.38E-03	1	4.38E-03	4.38E-03
$Si(OH)_4$	1.65E-03	0	0.00E+00	0.00E+00
Cl	2.06E-04	-1	-2.06E-04	2.06E-04
NO_3	4.10E-02	-1	-4.10E-02	4.10E-02
SO_4	6.13E-04	-2	-1.23E-03	2.45E-03
UO_2	4.20E-05	2	8.40E-05	1.68E-04
H	1.45E-04	1	1.45E-04	1.45E-04
OH	1.00E-10	-1	-1.00E-10	1.00E-10
CO_3	4.45E-05	-2	-8.90E-05	1.78E-04
	Sum:		0.0021	
	0.5 Sum:			0.0639
			CB / IS =	0.03

9,1 Batch			Charge Balance	Ionic Strength
	Conc.(M)	z	(z*M)	(z^2*M)
Ca	2.57E-04	2	5.14E-04	1.03E-03
K	6.67E-05	1	6.67E-05	6.67E-05
Na	2.45E-03	1	2.45E-03	2.45E-03
$Si(OH)_4$	7.22E-04	0	0.00E+00	0.00E+00
Cl	1.07E-04	-1	-1.07E-04	1.07E-04
NO_3	1.19E-03	-1	-1.19E-03	1.19E-03
SO_4	1.52E-04	-2	-3.04E-04	6.08E-04
UO_2	4.20E-06	2	8.40E-06	1.68E-05
H	1.04E-03	1	1.04E-03	1.04E-03
OH	1.00E-05	-1	-1.00E-05	1.00E-05
CO_3	1.04E-03	-2	-2.08E-03	4.16E-03
	Sum:		0.0004	
	0.5 Sum:			0.0053
			CB / IS =	0.07

6.5,10 Batch			Charge Balance	Ionic Strength
	Conc.(M)	z	(z*M)	(z^2*M)
Ca	9.74E-03	2	1.95E-02	3.90E-02
K	3.18E-04	1	3.18E-04	3.18E-04
Na	1.63E-03	1	1.63E-03	1.63E-03
$Si(OH)_4$	6.55E-04	0	0	0
Cl	2.79E-04	-1	-2.79E-04	2.79E-04
NO_3	1.48E-02	-1	-1.48E-02	1.48E-02
SO_4	4.52E-04	-2	-9.04E-04	1.81E-03
UO_2	4.20E-06	2	8.40E-06	1.68E-05
H	5.85E-03	1	5.85E-03	5.85E-03
OH	1.82E-08	-1	-1.82E-08	1.82E-08
CO_3	5.86E-03	-2	-1.17E-02	2.34E-02
	Sum:		-0.0004	
	0.5 Sum:			0.0436
			CB / IS =	-0.01

9,10 Batch			Charge Balance	Ionic Strength
	Conc.(M)	z	(z*M)	(z^2*M)
Ca	7.46E-04	2	1.49E-03	2.98E-03
K	1.06E-04	1	1.06E-04	1.06E-04
Na	1.13E-02	1	1.13E-02	1.13E-02
$Si(OH)_4$	4.87E-04	0	0	0
Cl	2.44E-04	-1	-2.44E-04	2.44E-04
NO_3	5.45E-04	-1	-5.45E-04	5.45E-04
SO_4	2.99E-04	-2	-5.98E-04	1.20E-03
UO_2	4.20E-06	2	8.40E-06	1.68E-05
H	9.53E-03	1	9.53E-03	9.53E-03
OH	1.00E-05	-1	-1.00E-05	1.00E-05
CO_3	1.04E-02	-2	-2.08E-02	4.16E-02
	Sum:		0.0002	
	0.5 Sum:			0.0337
			CB / IS =	0.01

V. Measured ion concentrations for transport experiments using IC and ICP, with corresponding charge balance and ionic strength calculations.

4,10 Column			Charge Balance	Ionic Strength
	Conc.(M)	z	(z*M)	(z^2*M)
Ca	1.15E-04	2	2.30E-04	4.60E-04
K	1.10E-04	1	1.10E-04	1.10E-04
Na	1.13E-02	1	1.13E-02	1.13E-02
$Si(OH)_4$	3.29E-04	0	0	0
Cl	3.67E-04	-1	-3.67E-04	3.67E-04
NO_3	9.88E-03	-1	-9.88E-03	9.88E-03
SO_4	5.00E-04	-2	-1.00E-03	2.00E-03
UO_2	4.20E-05	2	8.40E-05	1.68E-04
H	1.45E-04	1	1.45E-04	1.45E-04
OH	1.00E-10	-1	-1.00E-10	1.00E-10
CO_3	4.45E-05	-2	-8.90E-05	1.78E-04
	Sum:		0.0005	
	0.5 Sum:			0.0123
			CB / IS =	0.04

9,1 Column			Charge Balance	Ionic Strength
	Conc.(M)	z	(z*M)	(z^2*M)
Ca	1.15E-04	2	2.30E-04	4.60E-04
K	1.10E-04	1	1.10E-04	1.10E-04
Na	2.26E-03	1	2.26E-03	2.26E-03
$Si(OH)_4$	3.29E-04	0	0	0
Cl	3.67E-04	-1	-3.67E-04	3.67E-04
NO_3	1.24E-05	-1	-1.24E-05	1.24E-05
SO_4	5.00E-04	-2	-1.00E-03	2.00E-03
UO_2	4.20E-06	2	8.40E-06	1.68E-05
H	1.04E-03	1	1.04E-03	1.04E-03
OH	1.00E-05	-1	-1.00E-05	1.00E-05
CO_3	1.04E-03	-2	-2.08E-03	4.16E-03
	Sum:		0.0002	
	0.5 Sum:			0.0052
			CB / IS =	0.03

6.5,10 Column			Charge Balance	Ionic Strength
	Conc.(M)	z	(z*M)	(z^2*M)
Ca	1.15E-04	2	2.30E-04	4.60E-04
K	1.10E-04	1	1.10E-04	1.10E-04
Na	1.13E-02	1	1.13E-02	1.13E-02
$Si(OH)_4$	3.29E-04	0	0	0
Cl	3.67E-04	-1	-3.67E-04	3.67E-04
NO_3	4.06E-03	-1	-4.06E-03	4.06E-03
SO_4	5.00E-04	-2	-1.00E-03	2.00E-03
UO_2	4.20E-06	2	8.40E-06	1.68E-05
H	5.85E-03	1	5.85E-03	5.85E-03
OH	1.82E-08	-1	-1.82E-08	1.82E-08
CO_3	5.86E-03	-2	-1.17E-02	2.34E-02
	Sum:		0.0003	
	0.5 Sum:			0.0238
			CB / IS =	0.01

9,10 Column			Charge Balance	Ionic Strength
	Conc.(M)	z	(z*M)	(z^2*M)
Ca	1.15E-04	2	2.30E-04	4.60E-04
K	1.10E-04	1	1.10E-04	1.10E-04
Na	1.13E-02	1	1.13E-02	1.13E-02
$Si(OH)_4$	3.29E-04	0	0	0
Cl	3.67E-04	-1	-3.67E-04	3.67E-04
NO_3	1.24E-05	-1	-1.24E-05	1.24E-05
SO_4	5.00E-04	-2	-1.00E-03	2.00E-03
UO_2	4.20E-06	2	8.40E-06	1.68E-05
H	9.53E-03	1	9.53E-03	9.53E-03
OH	1.00E-05	-1	-1.00E-05	1.00E-05
CO_3	1.04E-02	-2	-2.08E-02	4.16E-02
	Sum:		-0.0010	
	0.5 Sum:			0.0327
			CB / IS =	-0.03